Design trade Study for a 4-meter off-axis primary mirror substrate and mount for the Habitable-zone Exoplanet Direct Imaging Mission

William R. Arnold, Sr.*[a], H. Philip Stahl[b]
[a]AI Solutions, Huntsville, Al.; [b]NASA MSFC, Huntsville, Al

ABSTRACT

An extensive trade study was conducted to evaluate primary mirror substrate design architectures for the HabEx mission baseline 4-meter off-axis telescope. The study's purpose is not to produce a final design, but rather to established a design methodology for matching the mirror's properties (mass and stiffness) with the mission's optical performance specifications (static dynamic wavefront error, WFE). The study systematically compares the effect of proven design elements (closed-back vs open-back vs partial-back; meniscus vs flat back vs shaped back; etc.), which can be implemented with proven space mirror materials (ULE and Zerodur), on static and dynamic WFE. Additionally, the study compares static and dynamic WFE of each substrate point design integrated onto three and six point mounts.

Keywords: HabEx, Primary Mirror Structural Design Studies, Mirror Suspension Geometry, Dynamic Performance.

1. INTRODUCTION

Habitable Exoplanet Imaging Mission (HabEx) is one of four missions under study for the 2020 Astrophysics Decadal Survey. Its goal is to directly image and characterize planetary systems in the habitable zone of Sun-like stars. Additionally, HabEx will perform a broad range of general astrophysics science enabled by 100 to 2500 nm spectral range and 3 x 3 arc-minute FOV. The baseline HabEx telescope is a 4-meter off-axis unobscured three-mirror-anastigmatic, diffraction limited at 400 nm with wavefront stability on the order of a few 10s of picometers.

The HabEx wavefront stability specification is driven by coronagraphy. Imaging an exoplanet, requires blocking 10^{10} of the host star's light. A coronagraph (with deformable mirrors) creates a 'dark hole' with < 10^{-10}contrast (Figure 1). But only if the primary mirror is ultra-smooth (< 5 nm rms) and ultra-stable (a few 10s of picometers). Static mid-spatial frequency error can reduce signal to noise and dynamic mid-spatial wavefront error (WFE) can introduce speckles into the dark hole. A number of coronagraphs are under consideration, each with its own WFE sensitivity. A leading candidate for HabEx is the Vector Vortex Coronagraph (VVC). Figure 2 (provided by Garreth Ruane) summarizes the maximum allowed aberration that each VVC 'charge' design can accept and still produce a 10^{-10} contrast dark hole. For example, the VVC Charge 4 can accept 800 pm of defocus but only 7 pm of trefoil. While the VVC-8 can accept 12,000 pm of defocus and 570 pm of trefoil. The most likely source of dynamic trefoil WFE is the primary mirror reacting against its support system in response to mechanical vibration.

The objective of this study is not to produce a final design, but rather to establish criteria for candidate 4-m off-axis primary mirror substrates and mount system designs. The study systematically compares the effect of proven design elements (closed-back vs open-back vs partial-back; meniscus vs flat back vs shaped back; etc.) on static and dynamic WFE. Additionally, it compares static and dynamic WFE of mirror point designs integrated onto three and six point mounts.

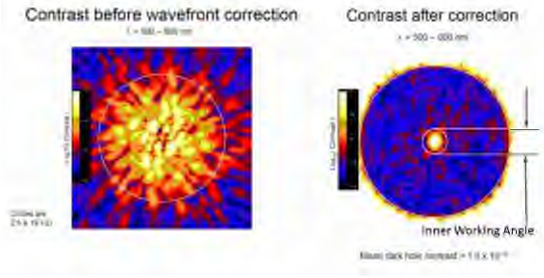

Figure 2 What a Coronagraph Does.

Aberration	Indices		Allowable RMS wavefront error (nm) per mode			
			charge 4	charge 6	charge 8	charge 10
Tip-tilt	1	±1	1.1	5.9	14	26
Defocus	2	0	0.8	4.8	12	28
Astigmatism	2	±2	0.0067	1.1	0.90	5
Coma	3	±1	0.0062	0.66	0.82	5
Spherical	4	0	0.0048	0.51	0.73	6
Trefoil	3	±3	0.0072	0.0063	0.57	0.67
2nd Astig.	4	±2	0.0060	0.0060	0.67	0.73
2nd Coma	5	±1	0.0036	0.0048	0.69	0.85
2nd Spher.	6	0	0.0025	0.0027	0.84	1
Quadrafoil	4	±4	0.0078	0.0080	0.0051	0.53
2nd Trefoil	5	±3	0.0051	0.0056	0.0043	0.72
3rd Astig.	6	±2	0.0023	0.0035	0.0034	0.81
3rd Coma	7	±1	0.0018	0.0022	0.0036	1.18
3rd Spher.	8	0	0.0010	0.0018	0.0033	1.49

Garreth Ruane, June 2017

not rejected
first-order rejection
> first-order rejection

Figure 1 Allowable SFE in terms of Zernike Coefficients

Arnold, Willian R. and H. Philip Stahl, "Design trade Study for a 4-meter off-axis primary mirror substrate and mount for the Habitable-zone Exoplanet Direct Imaging", UV/Optical/IR Space Telescopes and Instruments, 10398, Paper 7, San Diego, 2017.

2. STUDY GOALS AND METHODOLOGY

2.1 Study Goal

The goal of this study is to develop a methodology for evaluating the suitability of a candidate primary mirror assembly design for the HabEx mission. Suitability primarily depends on the wavefront error shape and amplitude produced by the mirror assembly when exposed to an expected vibration spectrum: how many picometers of defocus or trefoil or hexafoil, etc. Suitability also depends on total mass of the mirror assembly: ideally less than about 3000 kg.

For each design studied, its static gravity sag WFE is calculated and two different modal analyzes performed. Both modal analysis calculated the dynamic response of each design (both free-free and mounted) to a 1.0 Newton harmonic force applied over a range from 1 to 400 Hz. The first analysis applies the force normal to the mirror surface. This analysis is called 'on-axis'. The second analysis applies the force normal to the optical axis, which in HabEx is at approximately a 7-degree tilt angle relative to the surface normal. This analysis is called 'off-axis'. As one might expect the 'on-axis' performance is highly symmetric and the 'off-axis' performance as translational cross terms. For each modal analysis, translational (UX, UY, UZ) and rotational (TX, TY, TZ) response are calculated. The peak UZ (optical surface displacement direction) harmonic response is identified and ploted along with other significant modal responses (Figure 3). Finally, the peak UZ response is decomposed into Zernike Coefficients (Figure 4). PLEASE NOTE: because we are using a unit harmonic force, the absolute amplitudes are not meaningful in these results, only the relative proportions are applicable.

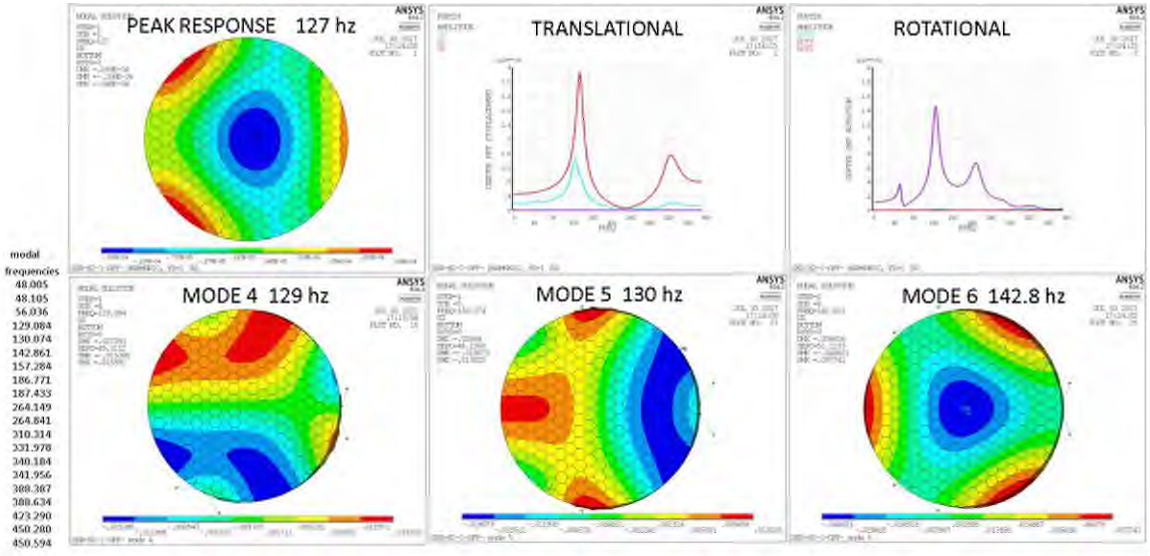

Figure 3: Typical Harmonic Response, Global Transfer Functions and mode shapes in frequency range of peak response.

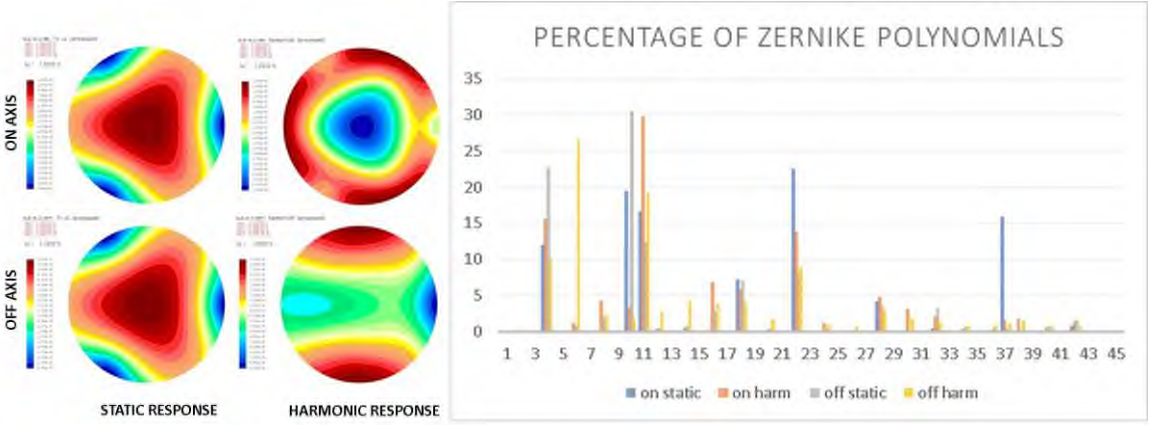

Figure 4: Using Zernike Coefficients to compare On-axis to Off-axis performance.

2.1 Study Methodology

A key feature of the study is its systematic comparison of design architectures. To minimize free variables, all mirror designs have a diameter if 4.2 meters and a thickness (at its maximum extent) of 42 cm. These dimensions were selected based upon available manufacturing capacities (or reasonable upgradeable capacities) and "practical" machining considerations. And, all designs have facesheets with the same thickness and core wall ribs have the same 'conservative' thickness. For the support systems, the axial stiffness and angles of the hexapod legs were keep equal (within rough limits). No attempt was made to adjust for a common frequency (stiffness-mass ratio). All loading was linear and the mean deflections are removed for optical (Zernike Coefficients) calculations to preserve the relative performance (static versus harmonic response). During the course of the study it became obvious that local attachment reinforcement (the region around the hexapod mirror attachment pads) plays a significant role in frequency and somewhat less in mode shape. The zone of reinforcement and "extra thickness" of that zone was kept constant for all cases.

All point designs considered by this study are traceable to published architectures (Figure 5) which can be manufactured via high Technology Readiness Level (TRL) processes. Based on their proven flight heritage, ULE and Zerodur mirrors were chosen for the study. The assumption is that closed-back ULE mirrors will be manufactured via the frit bond process and open-backed Zerodur mirrors will be manufactured via the ultra-lightweight pocket milling process.

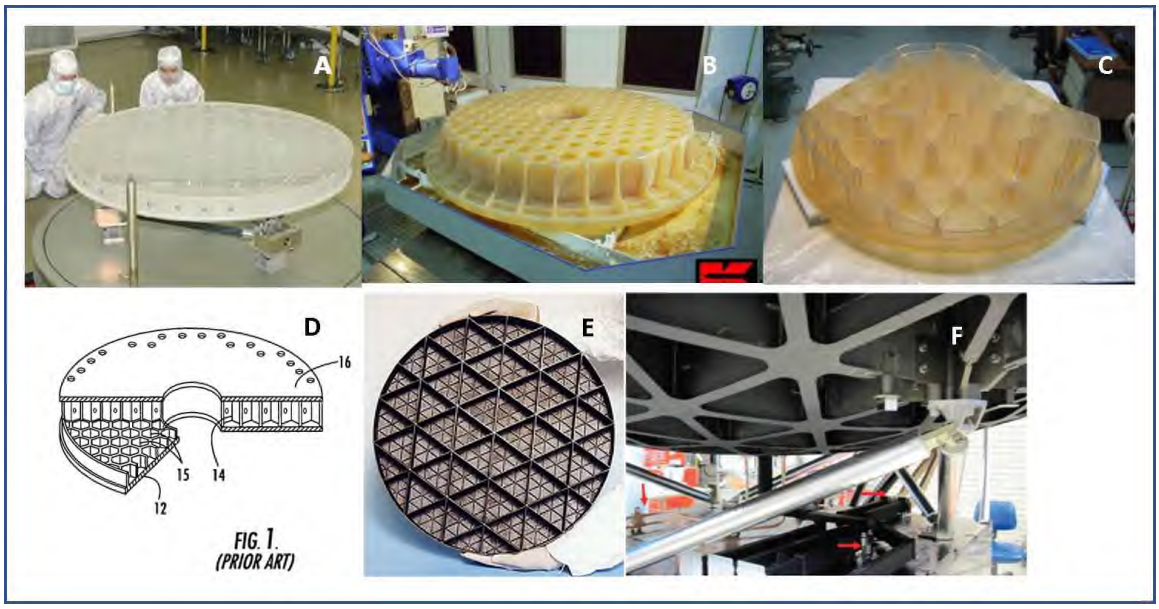

Figure 5: Published Trade Study Variants (some are patented and/or proprietary to a particular vendor).

For ULE designs, thickness is limited by what the waterjet process can easily cut from a solid boule to produce a lightweight core. At the 4.2-meter size, the minimum faceplate thickness was assumed to be controlled by handling equipment limitations during assembly rather than any ultimate thin plate possible. Some consideration was given to post frit machining, but the risk (cost if damaged after most of manufacturing cost already incurred for such extensive material removal) was considered unacceptable. Isogrid alternatives were again based upon a balance of risk during manufacture and realistic dimensions. As the main purpose of the study was to determine if other geometric variation contribute to the structural efficiency, these dimensions remain constant, only cell size (controls number of cuts required and has mass and stiffness influence) and suspension attachment numbers (three or six points) were varied. The cell sizes were picked as the best guess smallest practical and the largest practical before significant higher order wave front errors come into play (single cell plate span).

For Zerodur designs, the limiting dimensional factor is the volume of melt furnace capacity in current production, this can produce a cylindrical blank 4.2-meters in diameter by 420 millimeters deep. All the variant designs are constrained to fit within this volume. This limitation was the basis for the trade study, it is possible that Schott can increase production and/or offer alternative blank geometry, but the most established current limits were chosen for this study.

3. ULE® TRADE STUDIES

Figure 6 shows all of the design forms studied in the ULE® design study. Again, all designs have the same maximum thickness. For variant A, the thickness is uniform. For variants B & D, have their max thickness at the edge. This actually provides additional edge stiffness for the edge support system. Variant C has its max thickness in the center. Finally, in this analysis, when an isogrid was added to the front or to both front and back facesheets, the total mirror thickness was increased. The thickness of the front and back solid facesheets is constant for all variants.

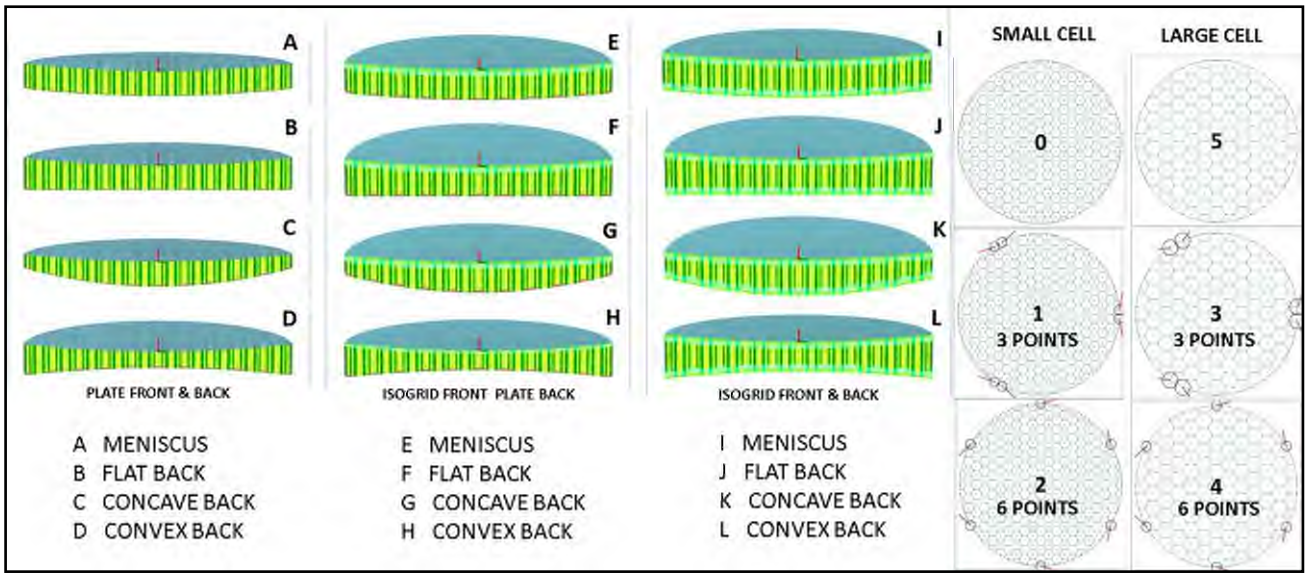

Figure 6: ULE® Trade Study Variants. The letters and numbers refer to particular models. All the configurations shown have both an on-axis and an off-axis version, with identical thickness parameters.

Potentially the most useful metric for quickly assessing the suitability of a given point design is its first mode frequency versus its mass (Figure 7 and 8). For a closed-back mirror, the meniscus variants consistently provided the highest first mode frequency. Marginally higher frequency performance can be achieved via adding isogrids, but at a significant mass penalty. The mirror designs all experience a significant frequency reduction when integrated with a three point or six point edge mount. This reduction might argue against edge mounting. The impact of edge mounting versus 80% or 65% mounting is explored in the Zerodur mirror trade study. Finally, while small cell cores may produce a smoother mirror (i.e. less quilting error) relative to a large cell core mirror, it has no stiffness advantage and it has a higher total mass.

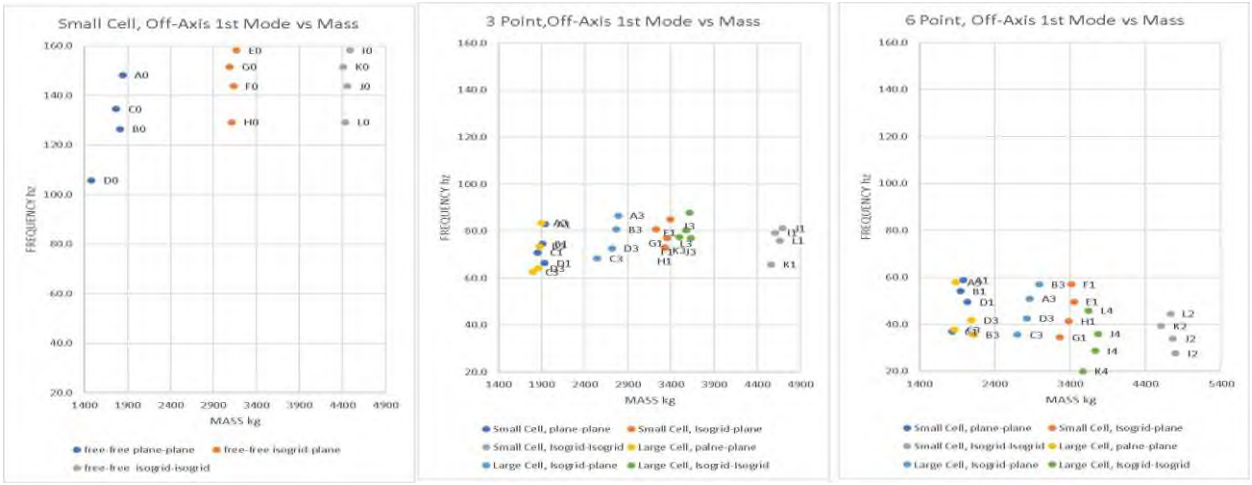

Figure 3 ULE Front and Back Plate Study. Uniform Thickness Plates and combinations with Isogrid Light-weighted Front and Back Plates. The three charts are free-free, 3 point supports and 6 point supports.

ON-AXIS

	-0 MASS	-0 1st	-1 MASS	-1 1st	-3 MASS	-3 1st	-2 MASS	-2 1st	-4 MASS	-4 1st
A	1836	149.4	1929	83.6	1883	84.1	1965	59.2	1873	58.1
B	1805	127.4	1897	75.2	1862	74.0	1933	54.4	2098	35.9
C	1755	135.5	1838	77.6	178	63.1	183	37.3	1851	38.4
D	1473	106.7	1920	66.8	1845	64.7	2032	49.7	2080	42.0
E	3151	150.0	3375	85.6	2776	87.2	3441	49.9	2850	51.4
F	3121	133.1	3340	75.5	2754	81.2	3405	57.2	2978	57.4
G	3070	140.0	3207	81.4	2644	78.5	3247	34.8	2685	35.8
H	3094	116.0	3309	73.5	2702	73.2	3374	41.5	2812	42.8
I	4466	159.2	4584	79.8	3596	88.4	4782	27.8	3713	28.9
J	4435	144.7	4675	81.7	3613	77.5	4747	34.0	3751	36.0
K	4385	152.6	4542	66.1	3477	78.0	4589	39.6	3548	20.0
L	4409	130.0	4644	76.6	3559	81.0	4715	44.7	3623	46.1

OFF-AXIS

	-0 MASS	-0 1st	-1 MASS	-1 1st	-3 MASS	-3 1st	-2 MASS	-2 1st	-4 MASS	-4 1st
A	1849	148.3	1941	82.9	1895	83.5	1976	58.8	1878	57.8
B	1818	126.5	1909	74.6	1874	73.5	1944	54.1	2120	35.6
C	1767	134.5	1850	70.9	1795	62.6	1838	36.9	1861	37.8
D	1483	105.8	1932	66.3	1857	64.1	2037	49.5	2091	41.7
E	3169	149.1	3391	85.0	2786	86.6	3450	49.6	2865	50.9
F	3138	132.2	3356	77.0	2764	80.7	3414	57.0	2992	57.0
G	3087	139.1	3223	80.7	2546	68.4	3263	34.5	2700	35.5
H	3111	115.2	3325	73.0	2717	72.7	3383	41.3	2826	42.5
I	4489	158.2	4605	79.3	3616	87.9	4796	27.6	3731	28.7
J	4458	143.8	4695	81.2	3629	77.0	4760	33.9	3766	35.9
K	4407	151.6	4563	65.8	3496	77.5	4607	39.3	3566	19.8
L	4431	129.2	4664	76.0	3577	80.4	4729	44.5	3641	45.8

NOTE: -5 Only ran for A On-Axis Case Mass= 1758 1st= 142.6

Figure 8: ULE® Mass versus First Mode Frequency in Tabular Form.

Appendix A shows the main results for each closed-back ULE substrate design variation. The figures are arranged to compare static to harmonic response for on-axis and off-axis mirrors under free-free, 3 points and 6 points support geometries attached to the perimeter of the mirror (no internal attachment point trade).

Finding #1: Because of the 7-degree tilt of the primary mirror relative to the optical axis, there is a noticeable difference in the on-axis vs off-axis static gravity sag. But this difference diminishes with the stiffer variants.

Finding #2: While there are differences, the on-axis and off-axis dynamic WFE shapes are extremely similar. Thus, an on-axis harmonic analysis may be an acceptable first order solution.

Finding #3: Obviously, the three point mount introduces a significant trefoil wavefront error – both static and dynamic. While the six point mount introduces a more circularly symmetric error. Given that the VVC-4 is relative insensitive to defocus and very sensitive to trefoil, a deliberate system engineering design choice might be to match a VVC-4 with a 6-point edge mount. However, a complete Zernike analysis of the dynamic WFE is required to determine its higher spatial frequency composition. Alternatively, given that the VVC-8 is insensitive to both defocus and trefoil, a system engineering design choice might be to match a VVC-9 with a 3-point mount.

4. ZERODUR© TRADE STUDIES

Zerodur mirrors present a design problem. Unlike ULE which can be built into a closed-back form but bonding multiple pieces together, Zerodur must be machined from a single solid boule. Thus, Zerodur mirrors are open-back mirrors. And open-back mirrors are inherently less stiff than closed back mirrors. Recently, there has been some process development for bonding Zerodur pieces to each other, but this work has not been validated for large mirrors. Thus, this study is constraining itself to open-back design forms.

Figure 9 shows all of the design forms studied in the Zerodur® design study. For these, the limiting dimensional factor is the capacity volume of the melt furnace. Currently, Schott can produce a cylindrical blank 4.2-m in diameter by 42-cm deep. All the variant designs are constrained to fit within this volume. It is possible that Schott can increase production and/or offer alternative blank geometry, but the most established current limits were chosen for this study. The purpose of the SOFIA design and the shaped back mirrors is to remove mass from the edge of the mirror (where it degrades

stiffness) and move that mass to portions of the mirror where added mass might increase stiffness. Each design form was investigated for the stiffness increase that could be gained from a moderate rear surface undercut and an extreme rear surface undercut. These undercuts increase stiffness by producing a partial rear back plate, or alternatively, by turning the core rib element into an 'I-beam'. Finally, the effect of mount system on performance was evaluated by attaching each design variant to the three point and six point mounts at its edge, 80% point and 65% point.

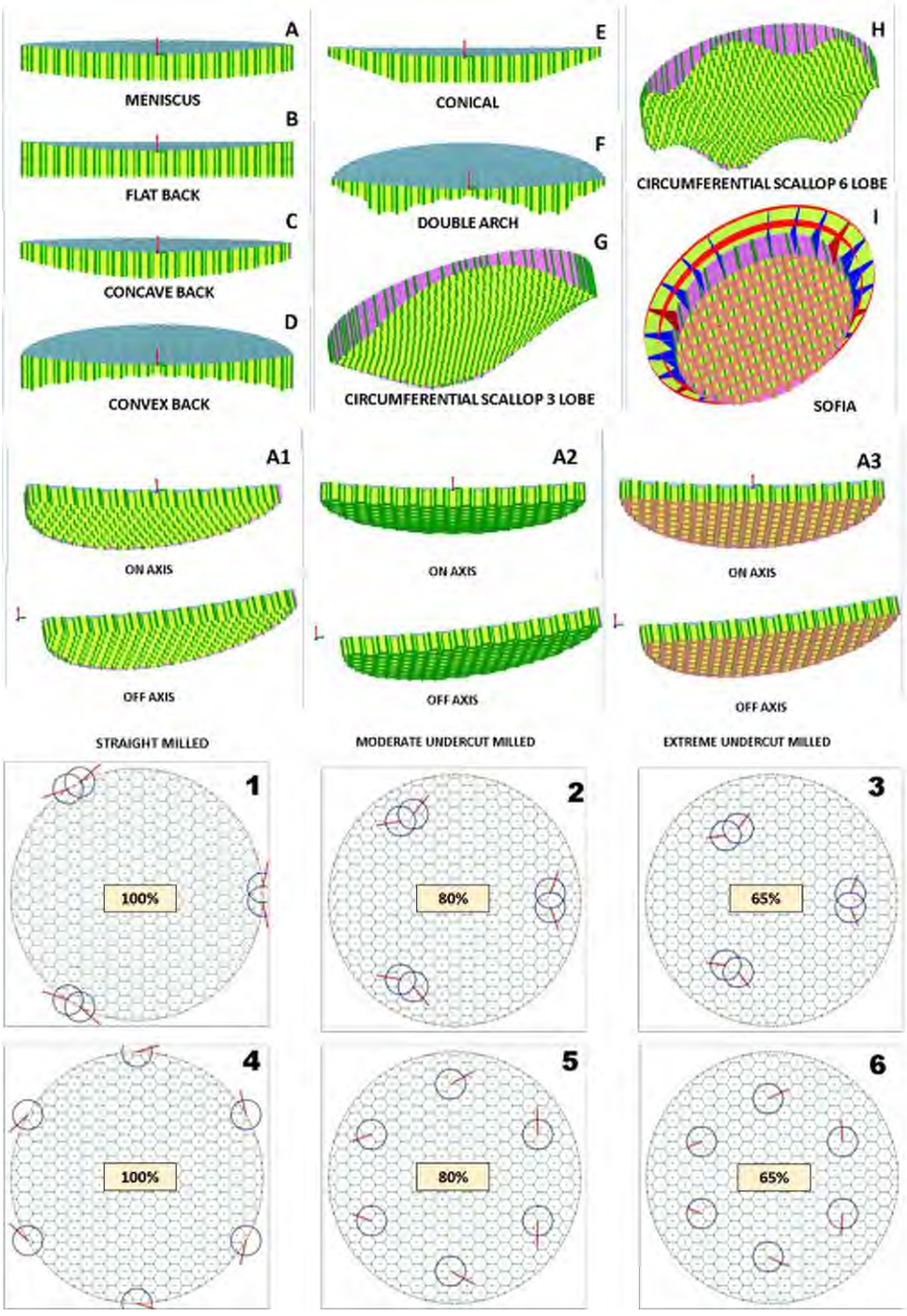

Figure 9: Zerodur Study: Each configuration has an on-axis and off-axis versions, with identical thickness parameters.

Again, the most useful metric for quickly assessing suitability of a given design is its first mode frequency versus mass (Figure 10). For an open-back mirror, the variants with the best stiffness to mass ratio are the flat-back and the meniscus shapes. Undercut milling produces a significant stiffer mirror, but at the cost of mass. However, all of the Zerodur substrate designs are well below the desired 3000 kg maximum. The extreme undercut SOFIA design has significantly higher stiffness and less mass than any other design.

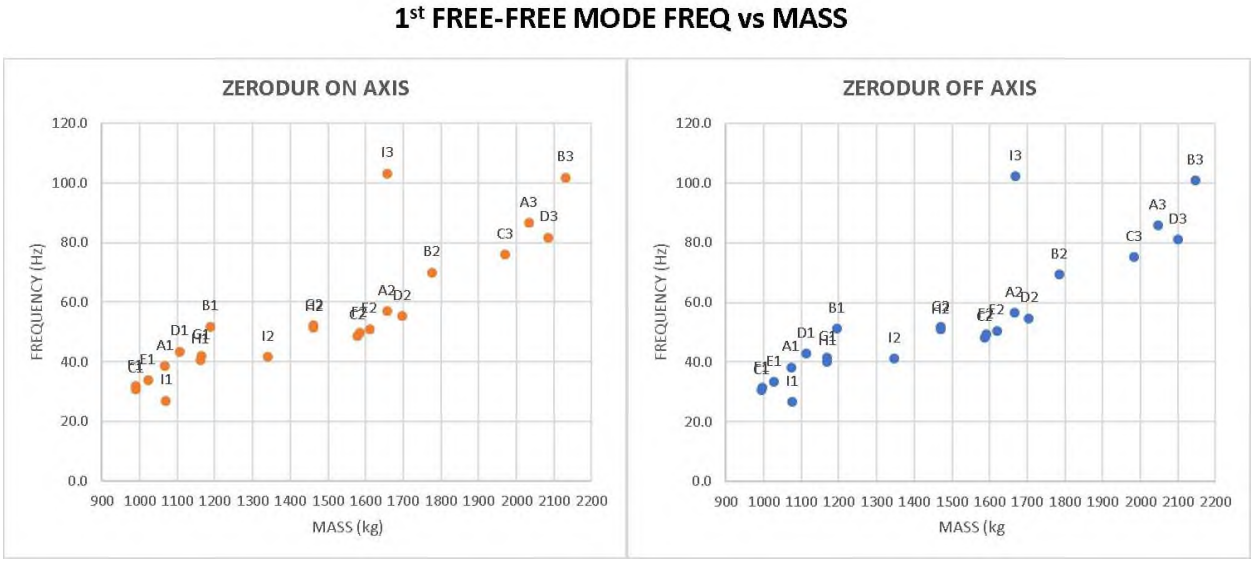

Figure 10: Zerodur design variants first mode frequency versus mass

Figure 11 shows how the UZ translation modal response moves to a higher frequency by adding undercuts. The top row shows the static 1-G gravity sag for the mirror in an on-axis and off-axis gravity orientation. The middle two rows show the translational (UX, UY, YZ) and rotational (TX, TY, TZ) response of the mirror system as a function of a 1 Newton harmonic driving force of frequency from 1 Hz to 400 Hz. The bottom row shows the peak dynamic wavefront error.

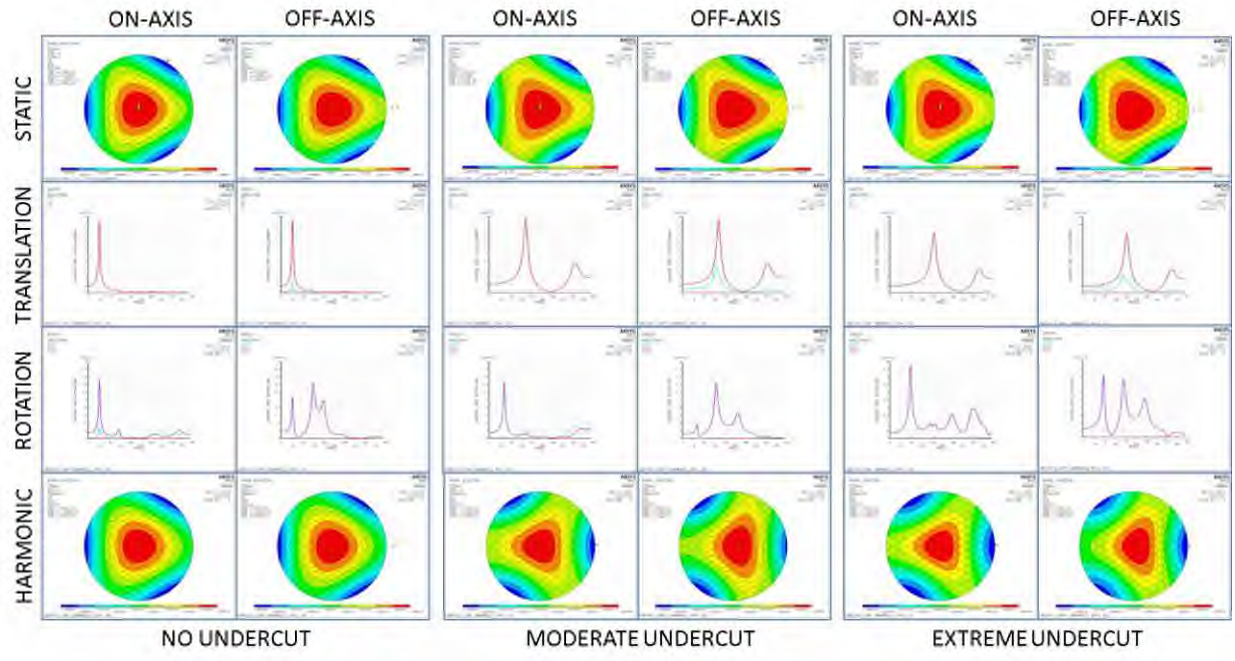

Figure 11: Effect of Pocket Milling Undercut on Stiffness

By comparison, Figure 12 shows how the UZ translation modal response is similarly shifted to higher frequency by increasing the core wall thickness. However, while the frequency increase is similar, the mass for a substrate with thicker core walls is obviously going to be higher than for undercut core walls.

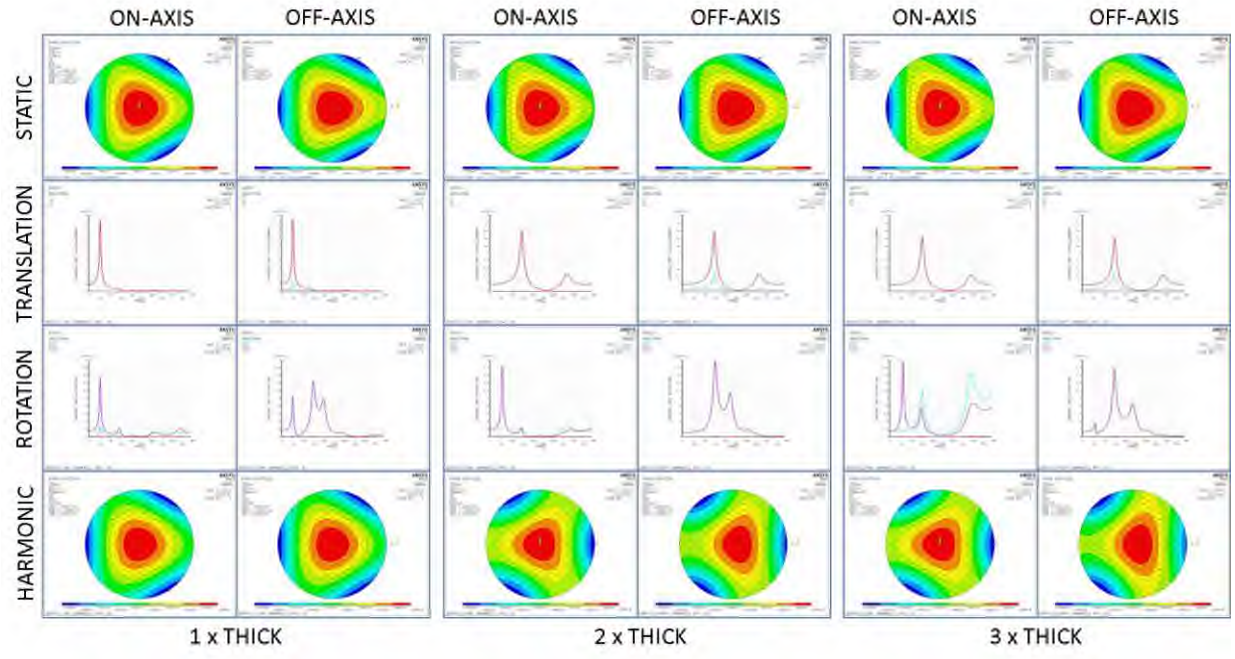

Figure 12: Effect Web Thickness of Straight (No Undercut) Pocket Milling on Stiffness

Because of the importance of dynamic trefoil error to the performance of candidate coronagraphs and the observation from the ULE study regarding differences in introduce error from the three point and size point mounts attached at the edge of the mirror, the Zerodur study investigated more mount options. It compared the static and dynamic surface error produced by mounting each open-back mirror variant (with and without undercuts) on to both three point and six point mounts at 100% (the outer mirror edge), 80% and 65% radial distances. The purpose of these studies is to investigate the effect of suspension attachment location and number of attachment points. The detailed results are in Appendix B:

- Figures B-1 to 3 show response of Flat Back variant with no, moderate and extreme undercut on 3-point mount
- Figures B-4 to 6 show response of Concave Back variant with no, moderate and extreme undercut on 3-point
- Figures B-7 to 9 show response of Convex Back variant with no, moderate and extreme undercut on 3-point
- Figures B-10 and 11 show response of Conical Back variant with no and moderate undercut on 3 point mount
- Figures B-12 and 13 show response of Double Arch Back variant with no and moderate undercut on 3 point
- Figures B-14 and 15 show response of 3-Node Scallop Back variant with no and moderate undercut on 3 point
- Figures B-16 and 17 show response of 6-Node Scallop Back variant with no and moderate undercut on 6 point
- Figures B-18 to B-20 show response of SOFIA Style variant with no, moderate and extreme undercut on 3 point

For nearly all of the mirror variants, moving the 3 point mount attachment to 65% reduced the dynamic trefoil error and increased the assembly peak mode response frequency – both of which are good for the vector vortex coronagarph.

Finally, Figure 13 shows the first ten mode shapes of a 42 cm thick, open-back meniscus Zerodur mirror when it is free-free, attached to a three point mount and attached to a six point mount at its edge (100% mount).

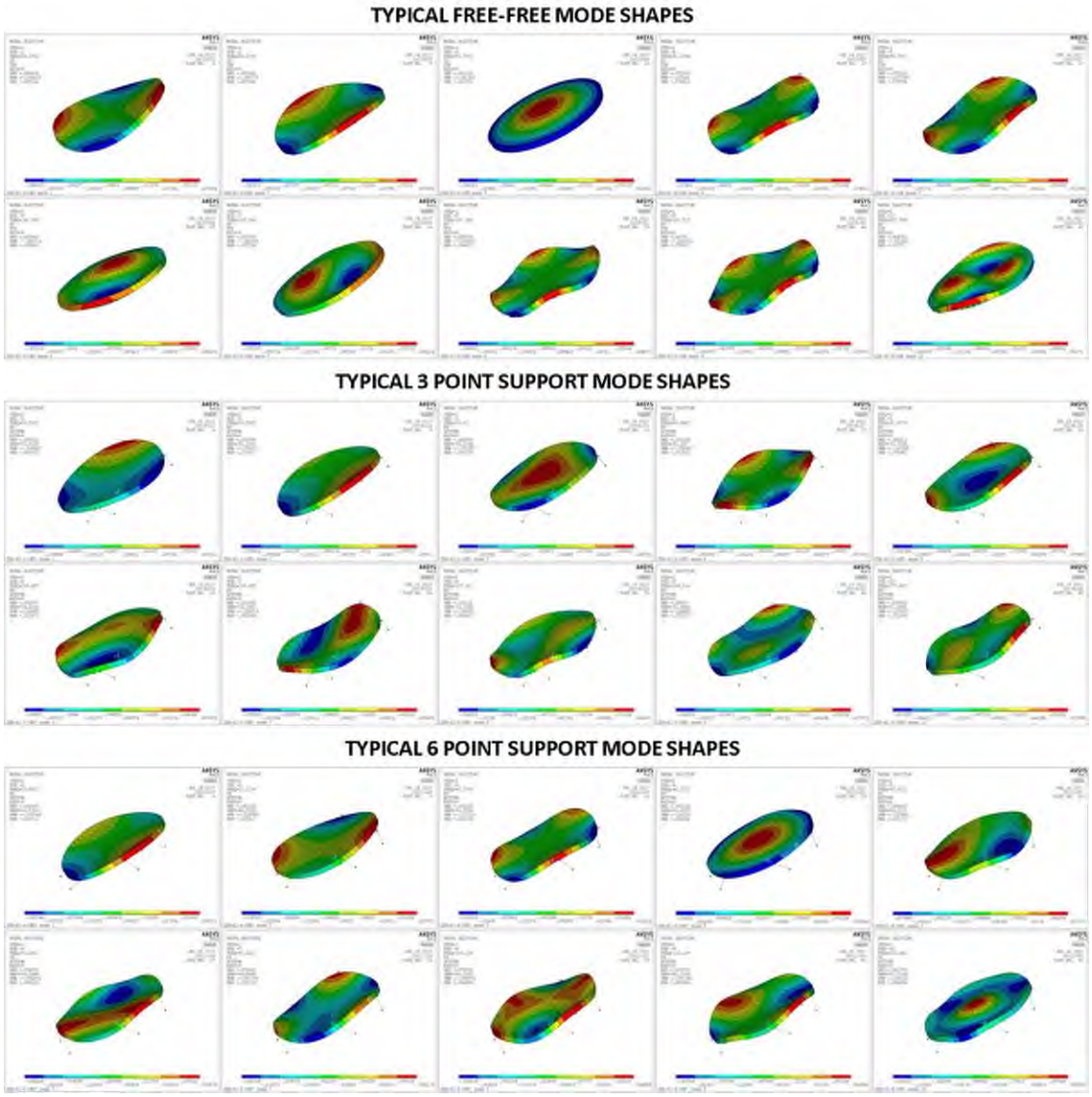

Figure 13: Effect of Support Geometry on Mode Shapes. The mirror is the same for all three configurations.

5. SUMMARIES AND CONCLUSIONS

An extensive trade study was conducted to evaluate primary mirror substrate design architectures for the HabEx mission baseline 4-meter off-axis telescope. The study's purpose is to establish a design methodology for matching the mirror's properties (mass and stiffness) with the mission's optical performance specifications (static dynamic wavefront error, WFE). The study systematically compares the effect of design elements (closed-back vs open-back vs partial-back; meniscus vs flat back vs shaped back; etc.). Additionally, the study compares static and dynamic WFE of each substrate point design integrated onto three and six point mounts.

This study has several preliminary findings. While there are differences, the on-axis and off-axis dynamic WFE shapes are extremely similar. Thus, an on-axis harmonic analysis may be an acceptable first order solution. Local structural reinforcement at the mount locations has a significant impact on dynamic performance. And, the stiffness enhancement from undercutting of Zerodur core walls is potentially worth the cost and risk. But, probably the most important finding is, that there are many potential design solutions and that, with proper attention to detail, it is possible to design a primary mirror assembly to specifically minimize dynamic wavefront errors to which the coronagraph is sensitive.

APPENDIX A: ULE Closed-Back Mirror Trade Study Results

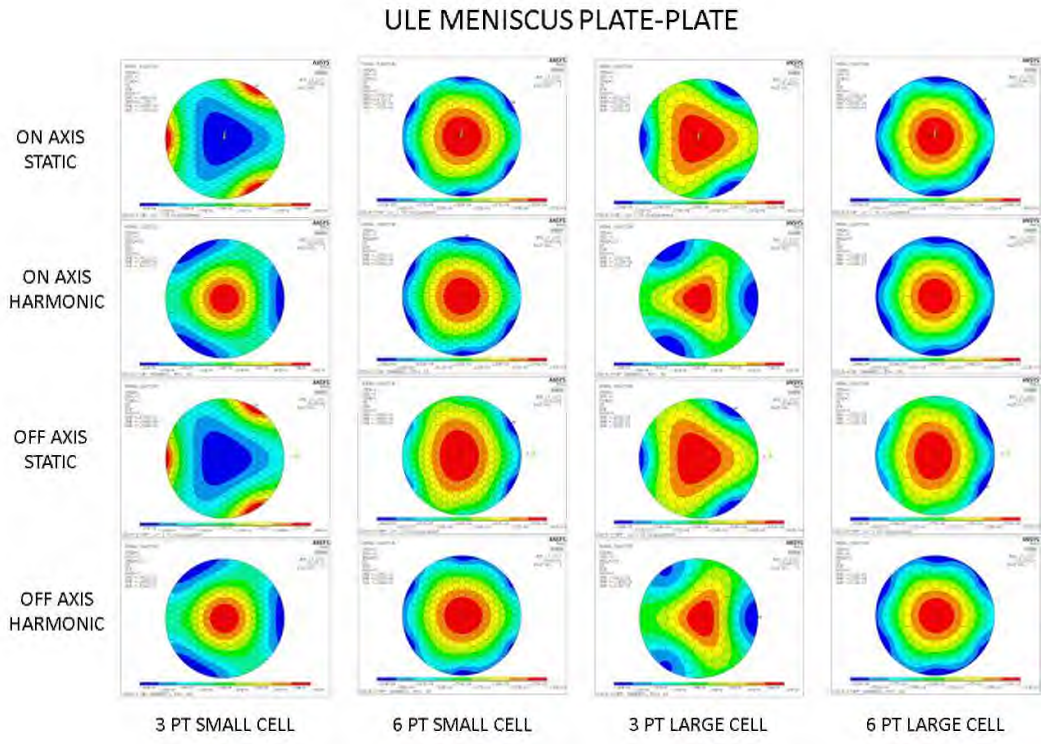

Figure A-1:4 Comparison Static vs Harmonic Response of Meniscus Back Mirrors.

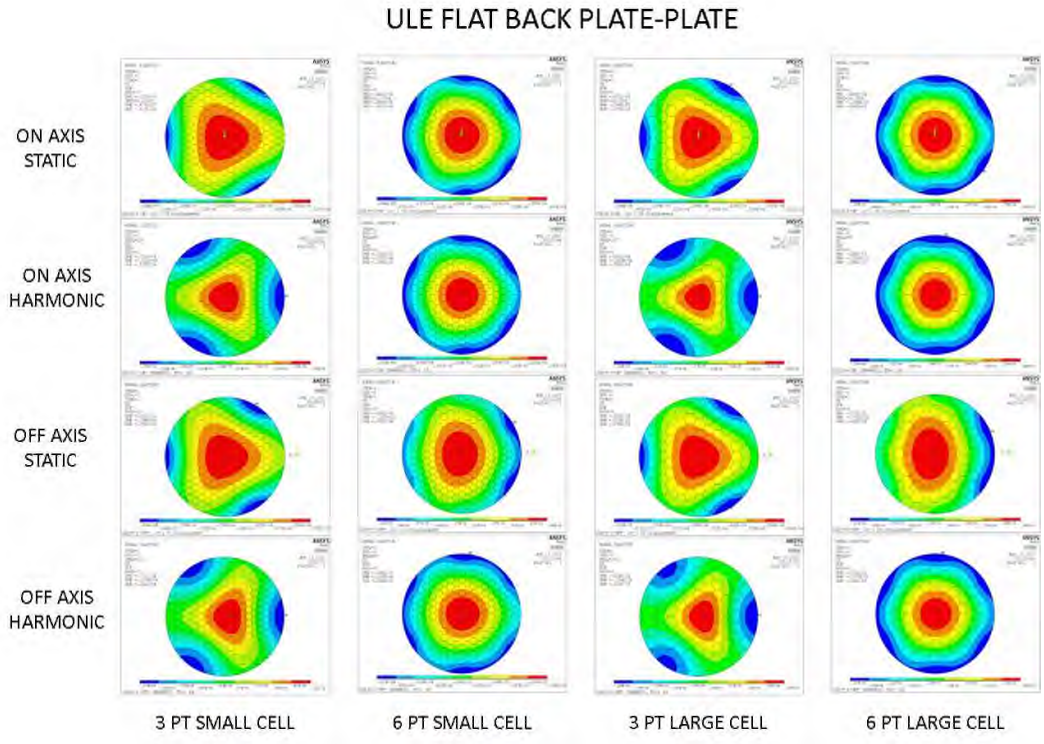

Figure A-2: Comparison Static vs Harmonic of Flat Back Mirrors

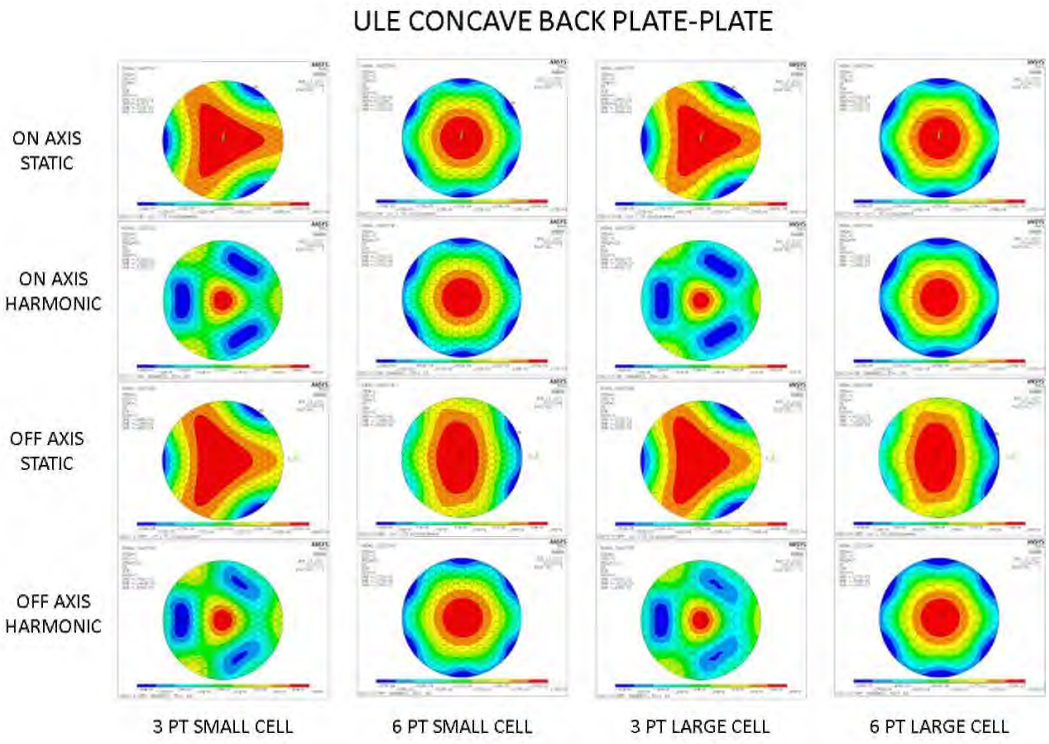

Figure A-3: Comparison of Static vs Harmonic Response of Concave Back Mirrors

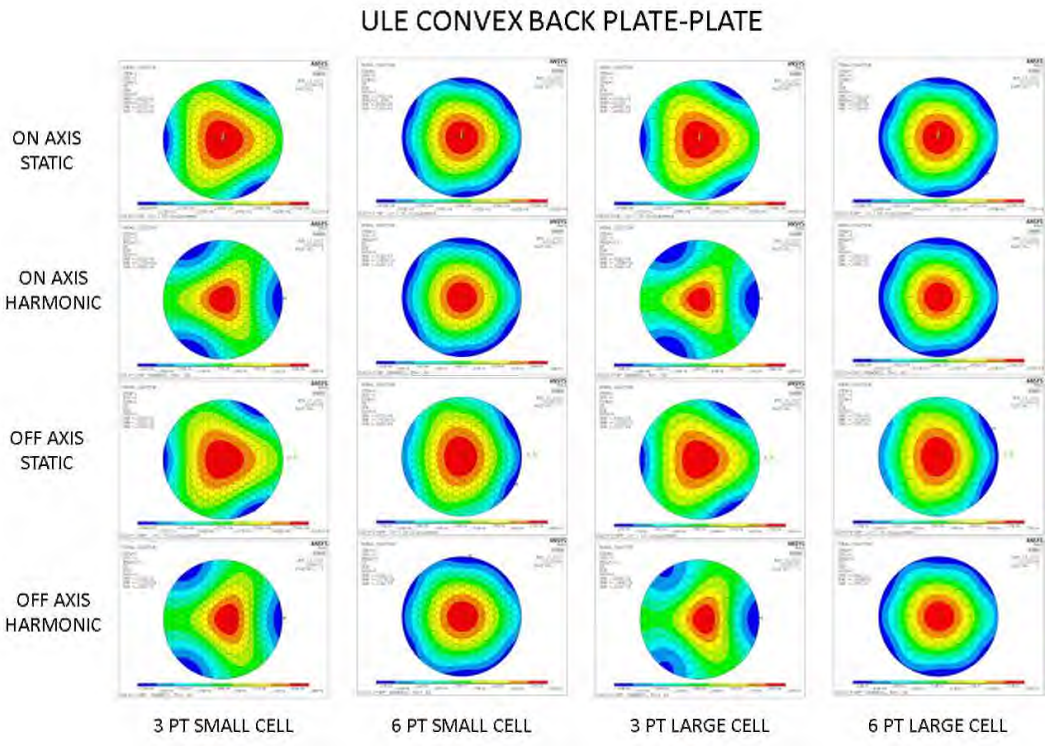

Figure A-4: Comparison of Static vs Harmonic Response of Convex Back Mirrors.

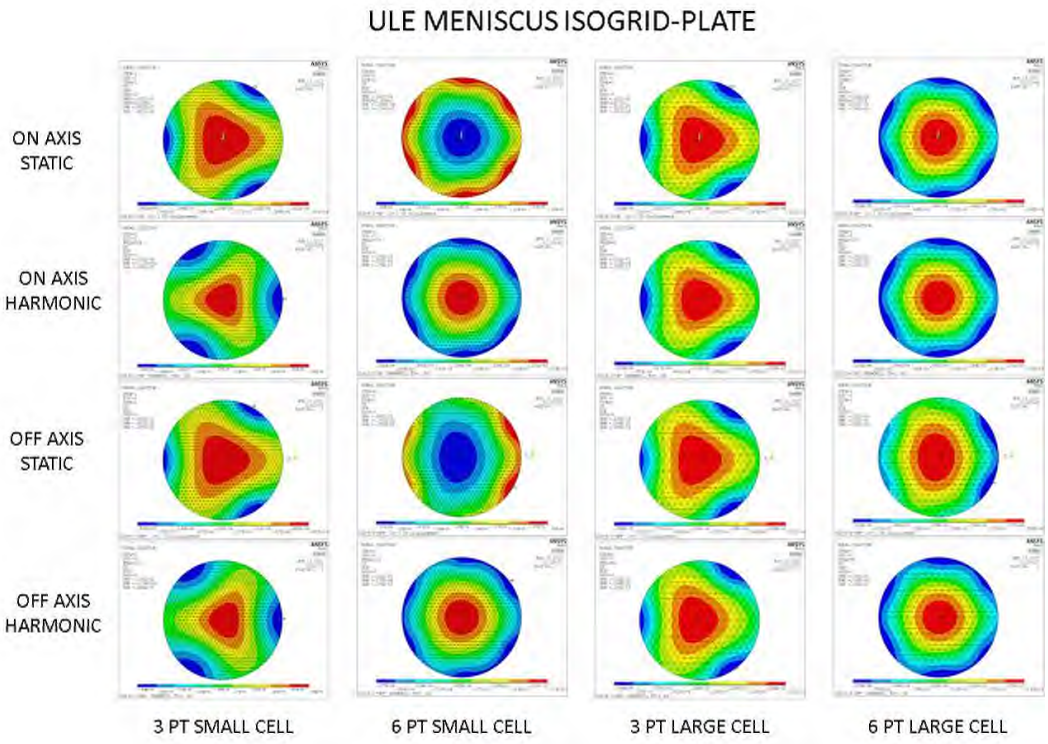

Figure A-5: Comparison of Static vs Harmonic Meniscus Back Mirrors.

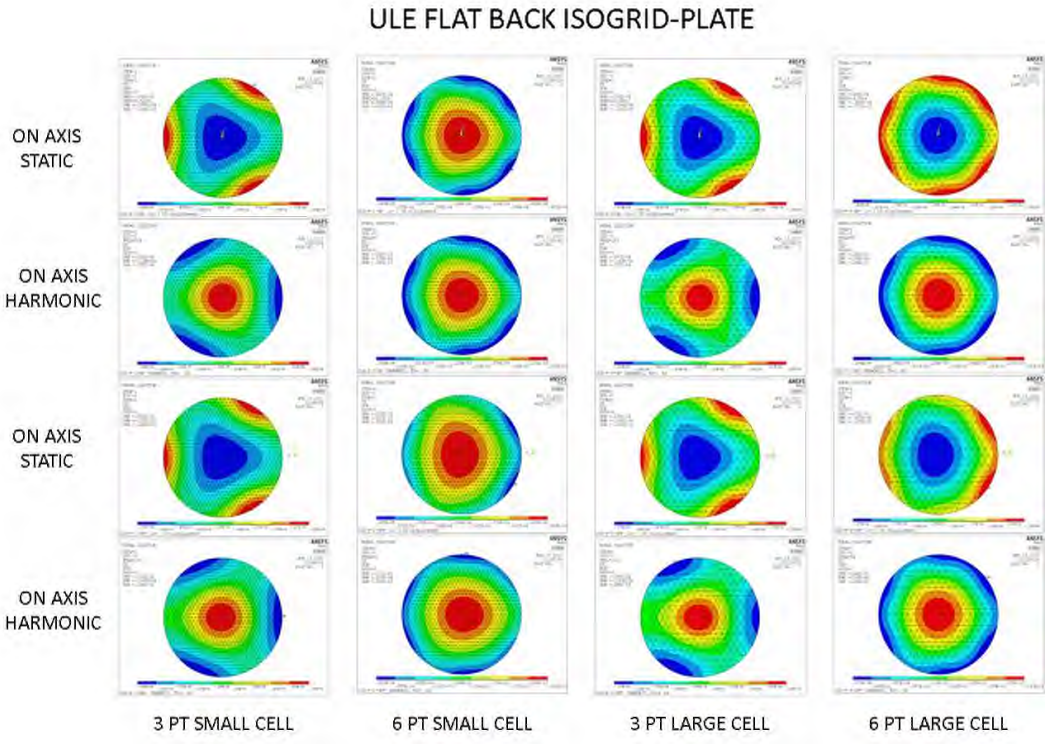

Figure A-6: Comparison of Static vs Harmonic Response of Flat Back Mirrors.

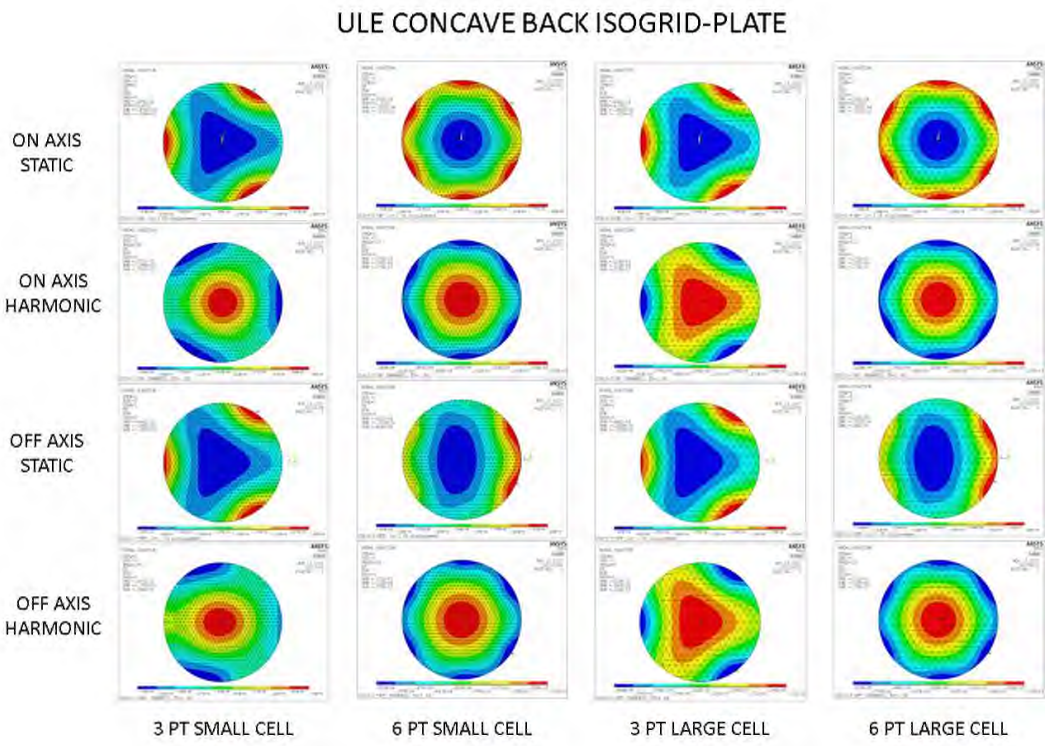

Figure A-7: Comparison of Static vs Harmonic Response of Concave Back Mirrors

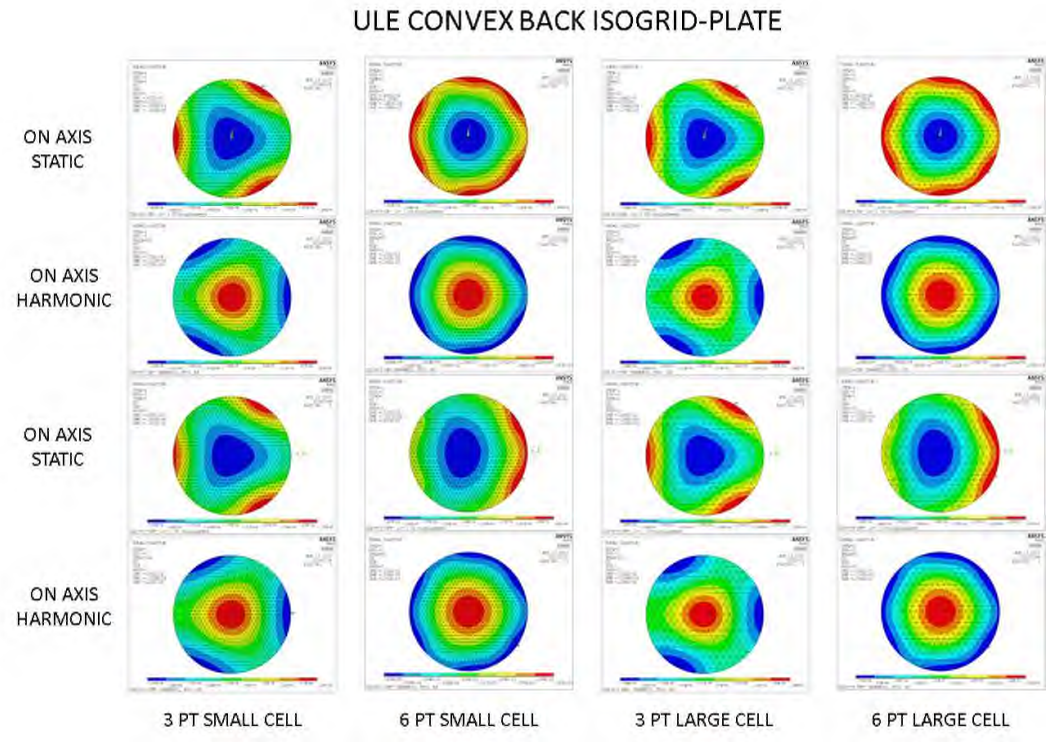

Figure A-8: Comparison of Static vs Harmonic Response of Convex Back Mirrors.

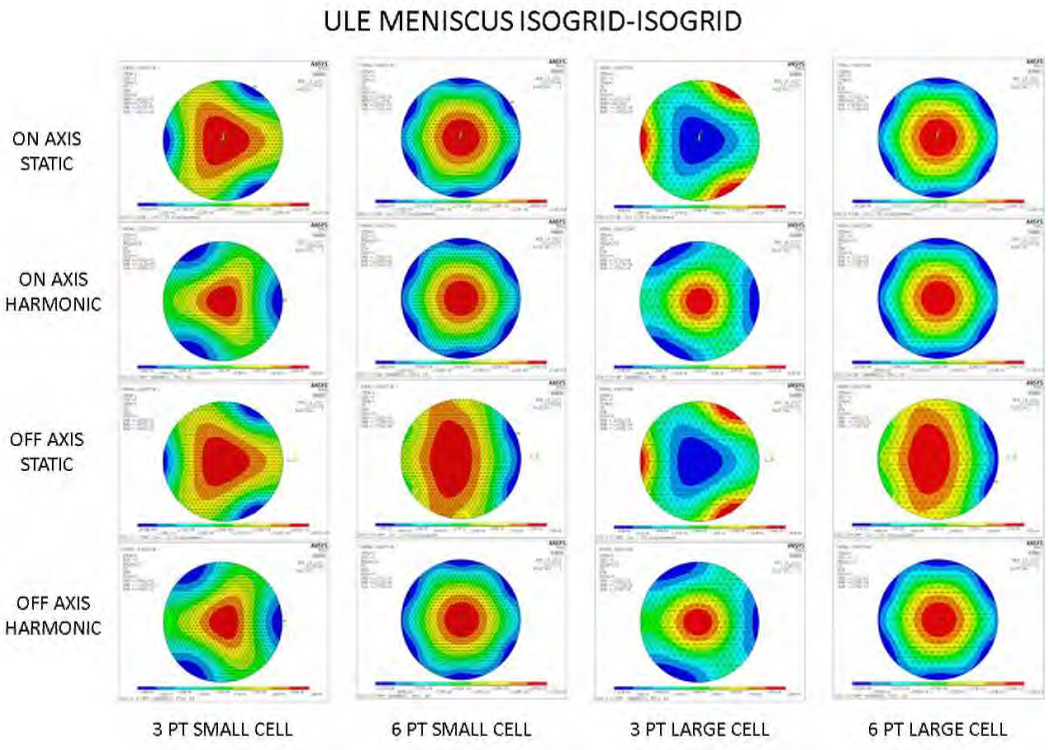

Figure A-9: Comparison of Static vs Harmonic Response of Meniscus Back Mirrors.

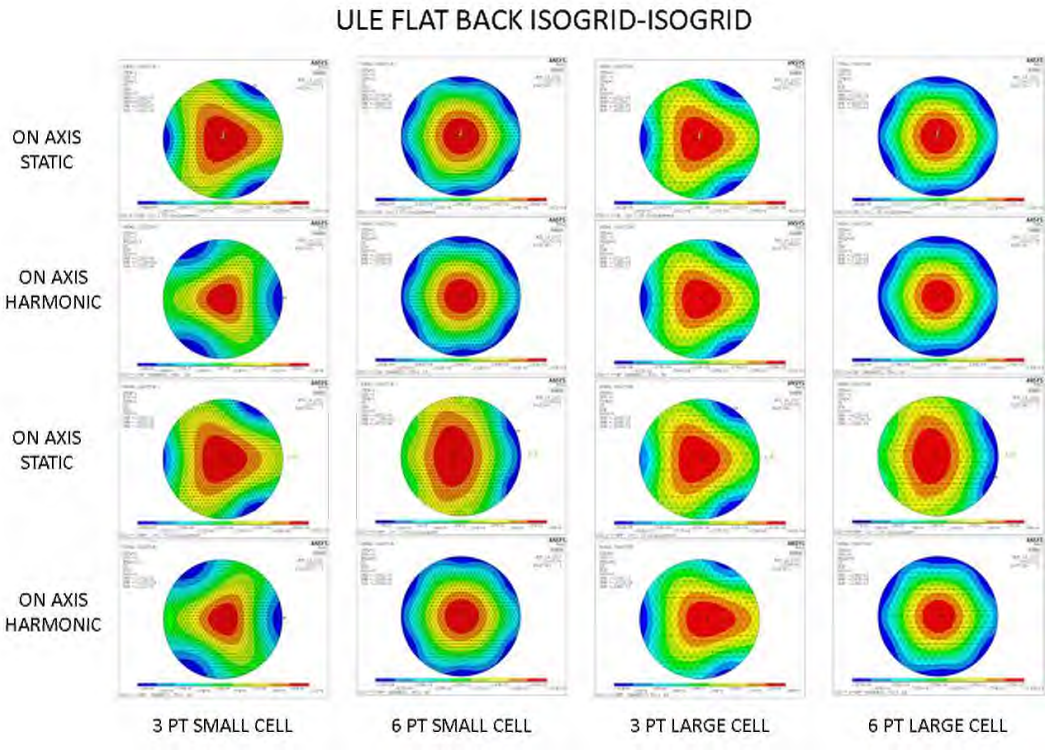

Figure A-10: Comparison of Static to Harmonic Response of Flat Back Mirrors.

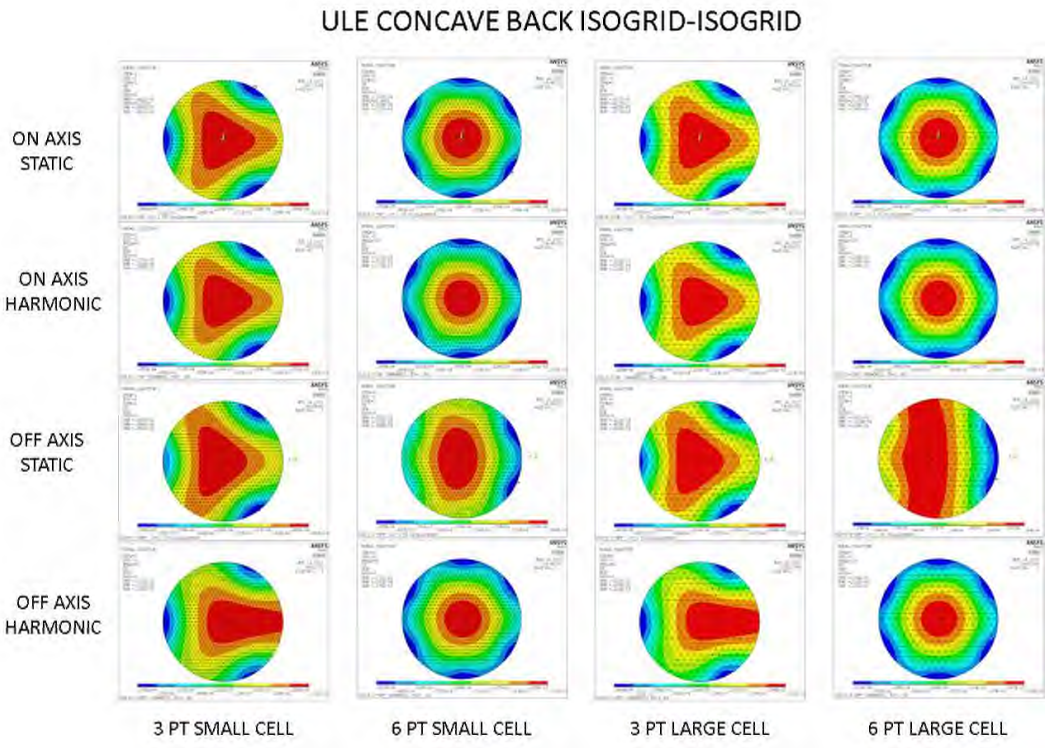

Figure A-11: Comparison of Static vs Harmonic Response of Concave Back mirrors.

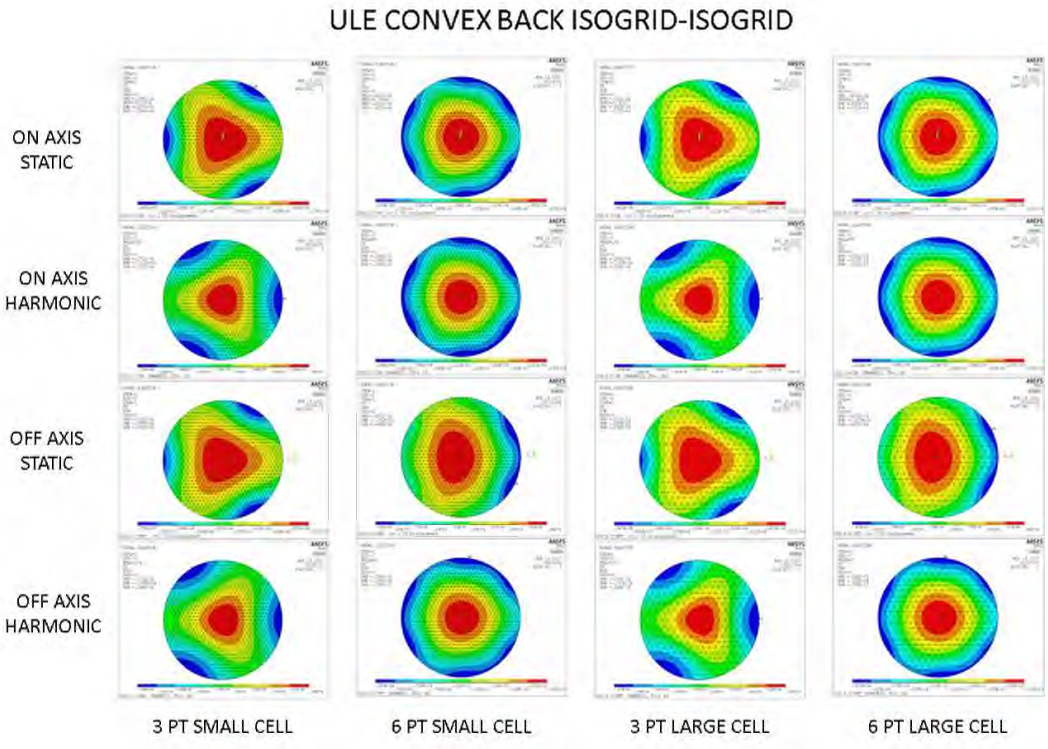

Figure A-12: Comparison of Static vs Harmonic Response of Convex Back Mirror.

APPENDIX B: Zerodur Open-Back Mirror Trade Study Results

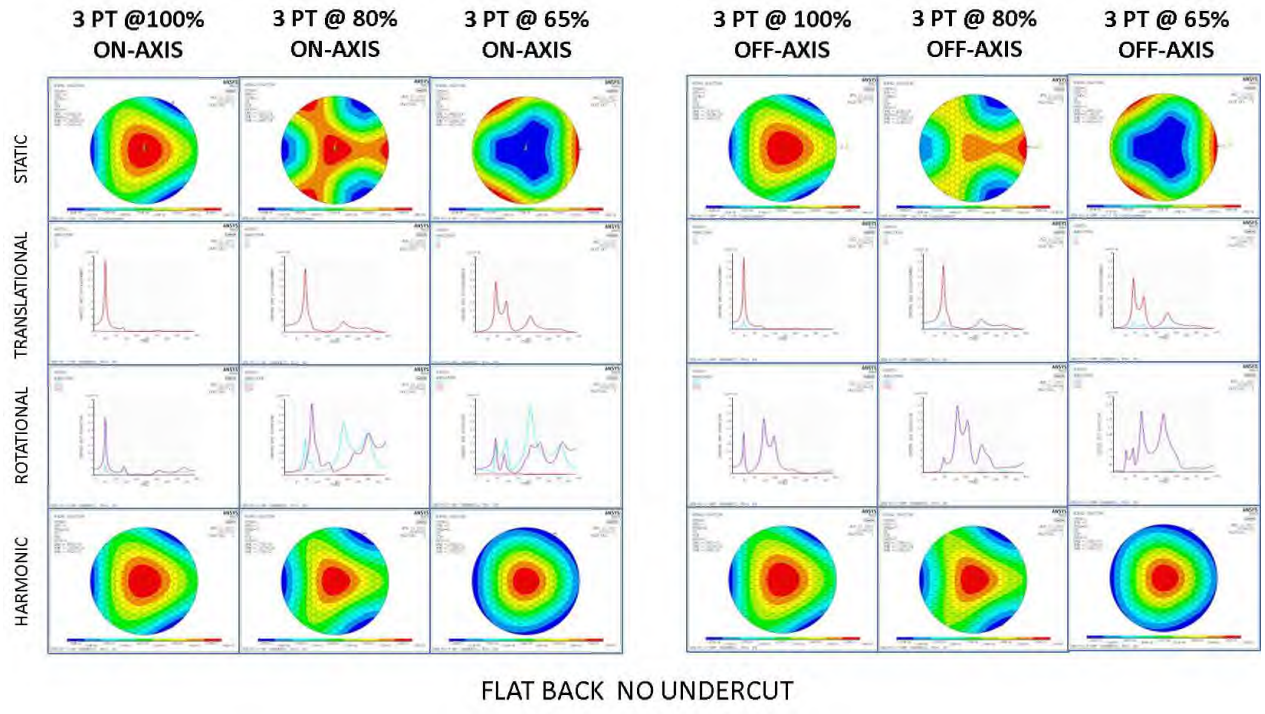

Figure B-1: Zerodur Trade Study #1: 3 Pt Support On-Axis vs Off-Axis

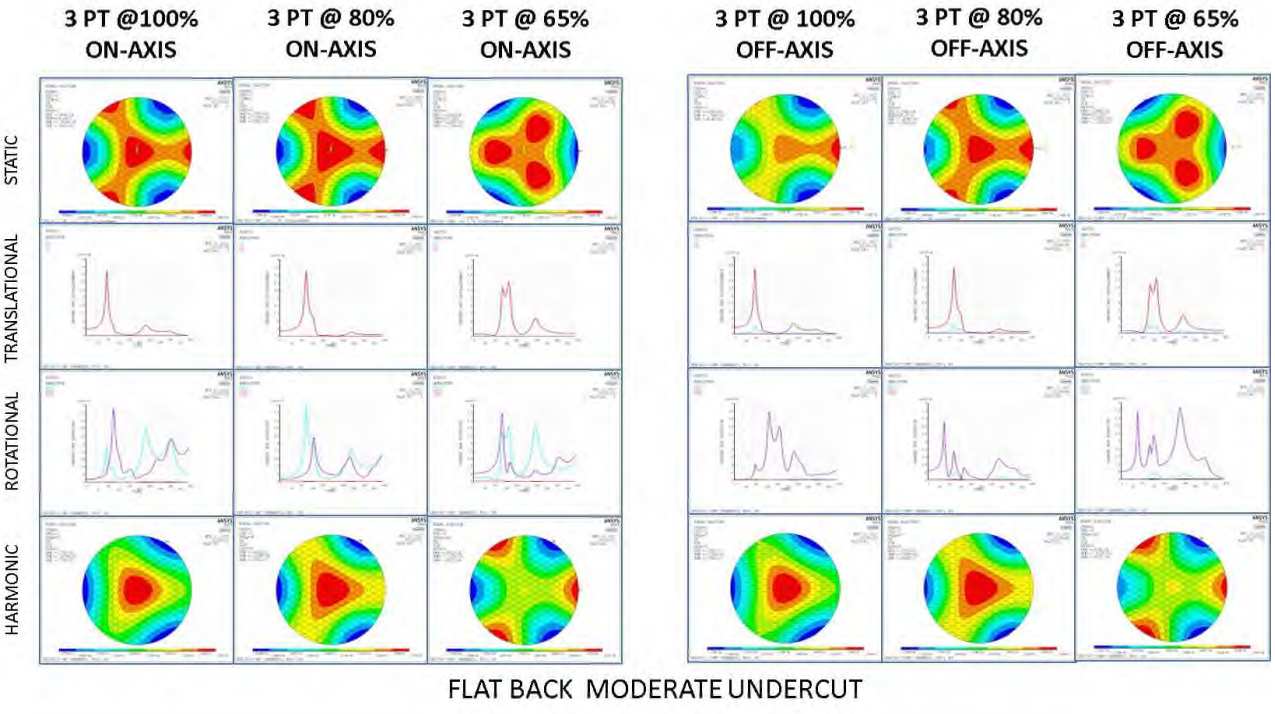

Figure B-2: Zerodur Trade Study #2: Flat Back, Moderate Undercut.

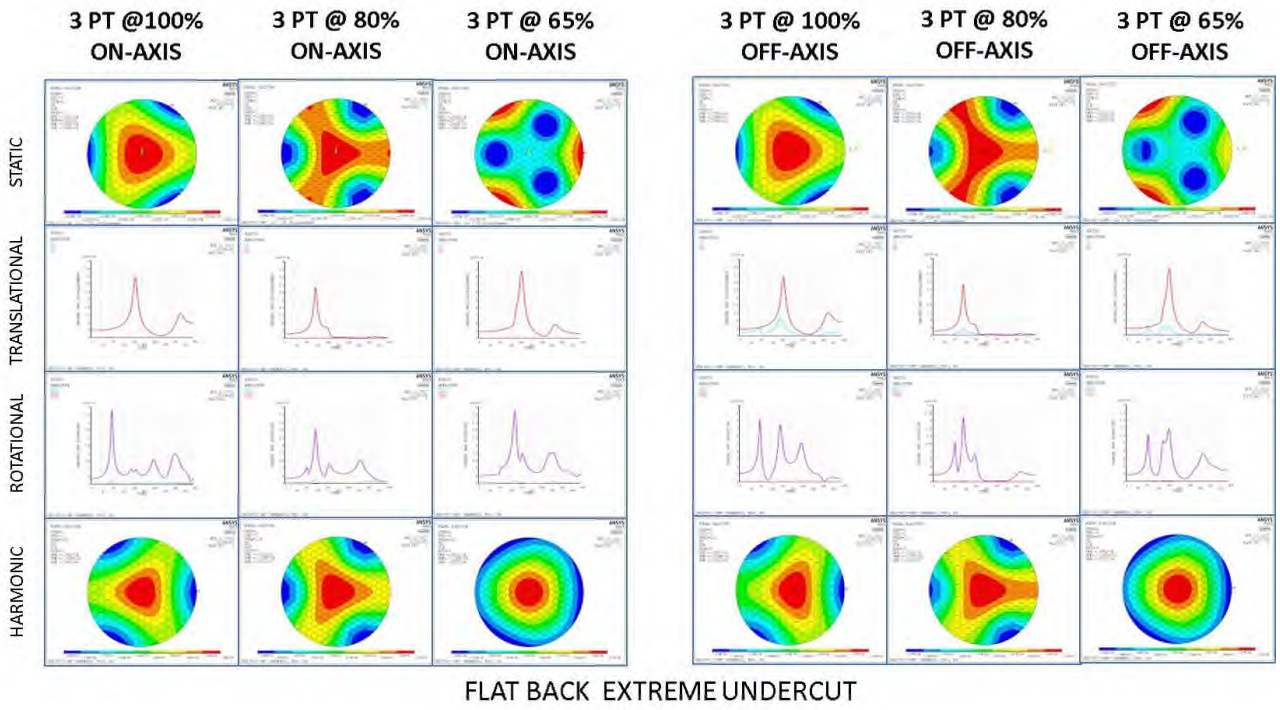

Figure B-3: Zerodur Trade Study #3

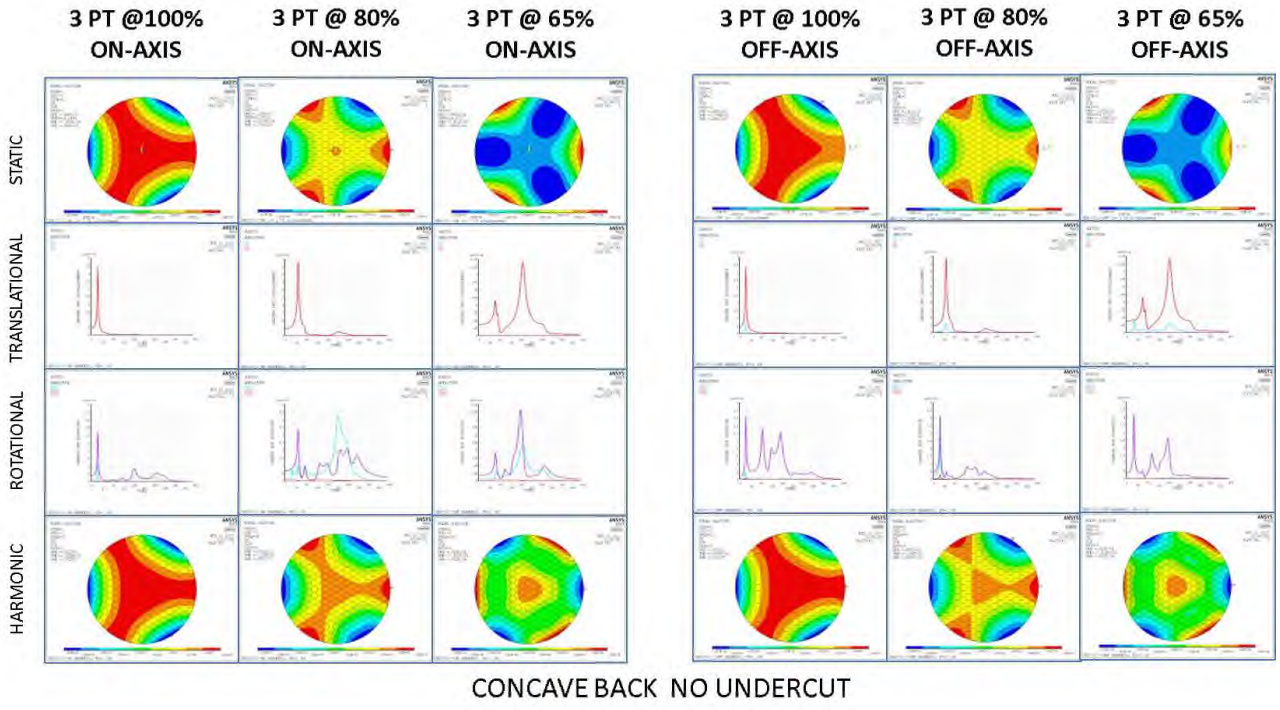

Figure B-4: Zerodur Trade Study #4

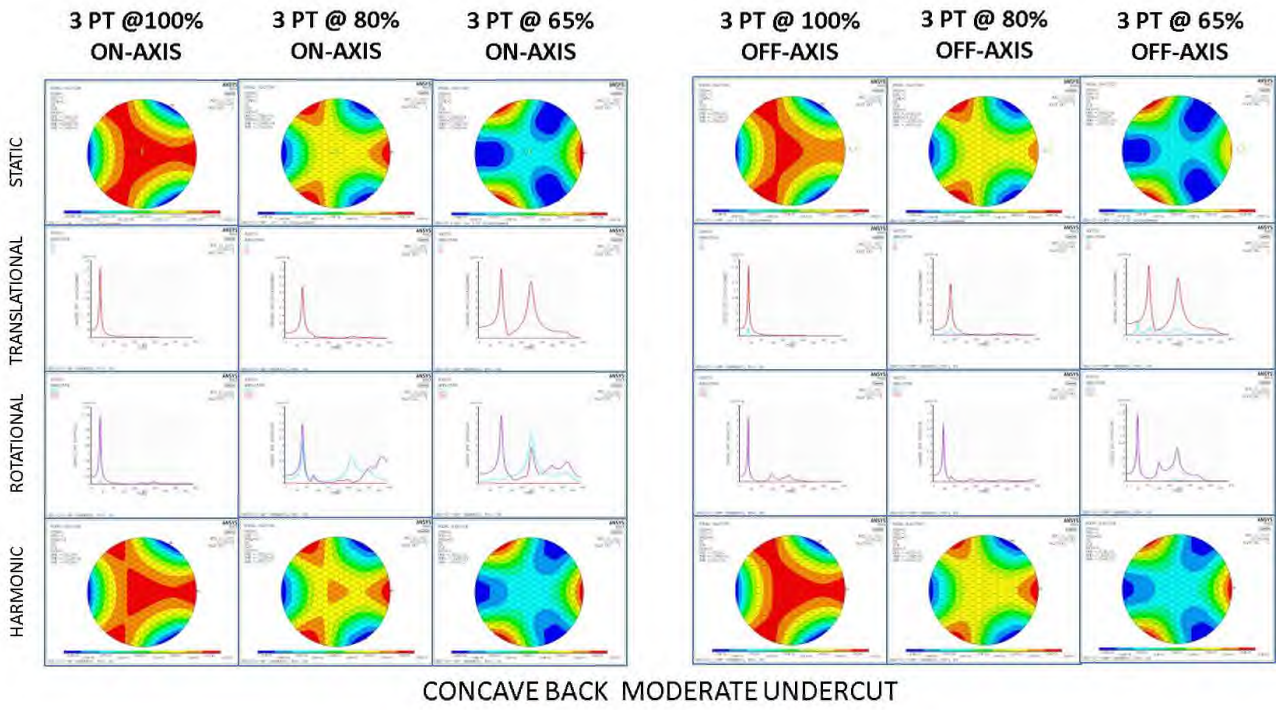

Figure B-5: Zerodur Trade Study #5

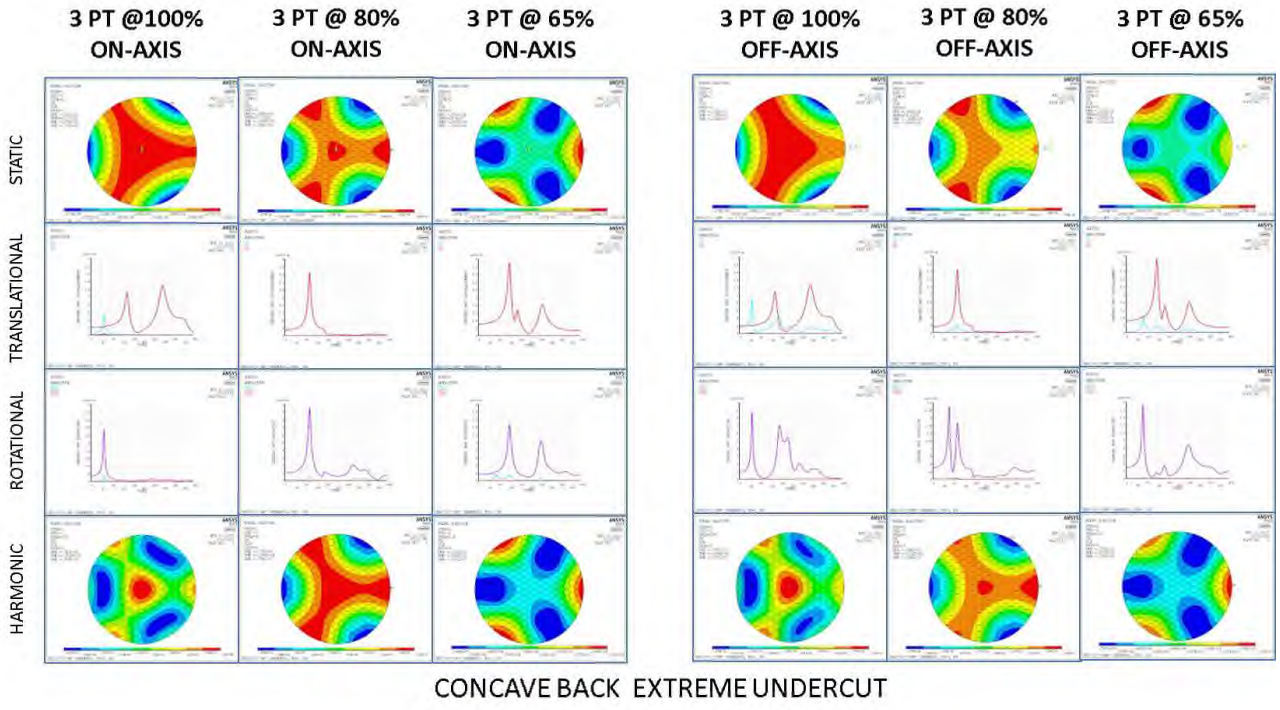

Figure B-6: Zerodur Trade Study #6

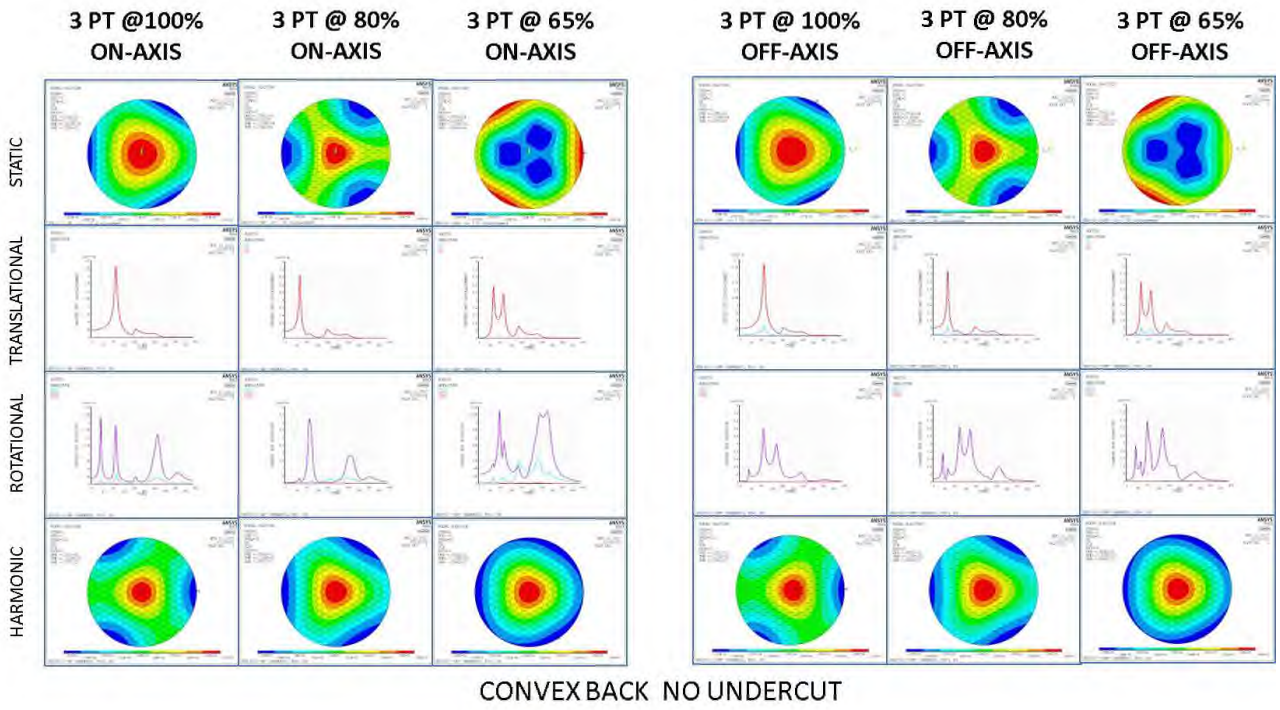

Figure B-7: Zerodur Tarde Study #7

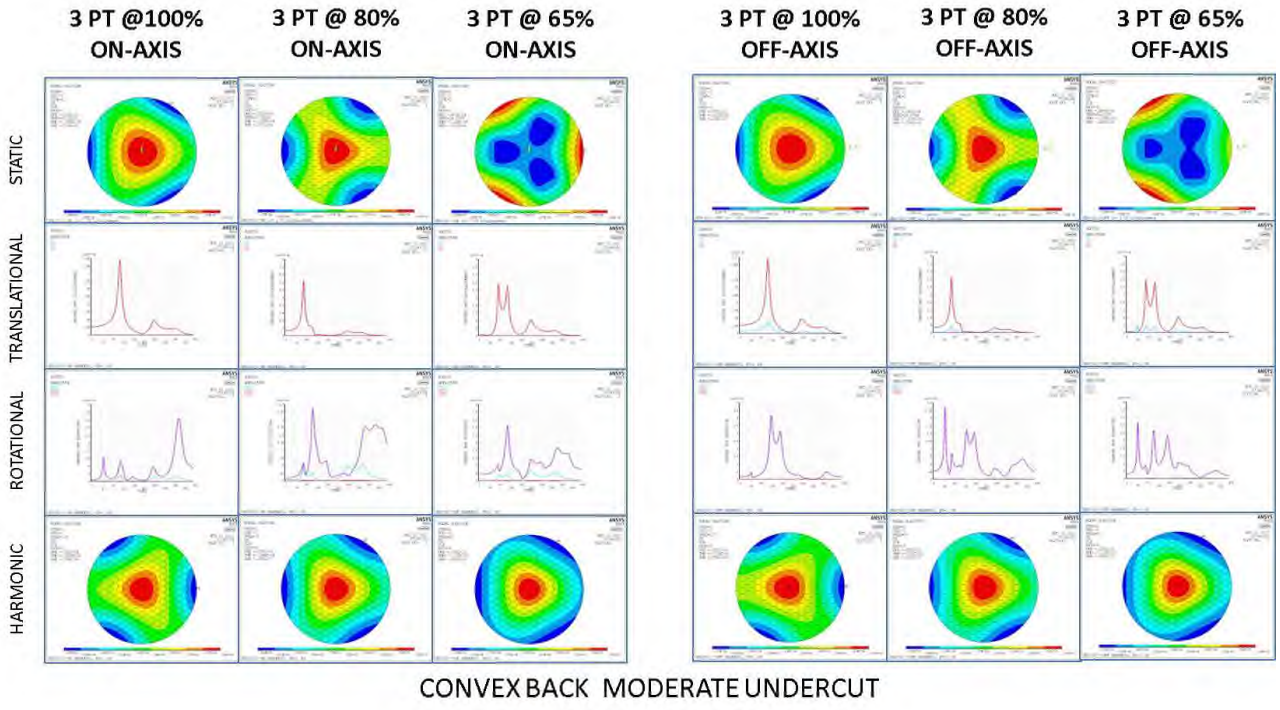

Figure B-8: Zerodur Trade Study #8

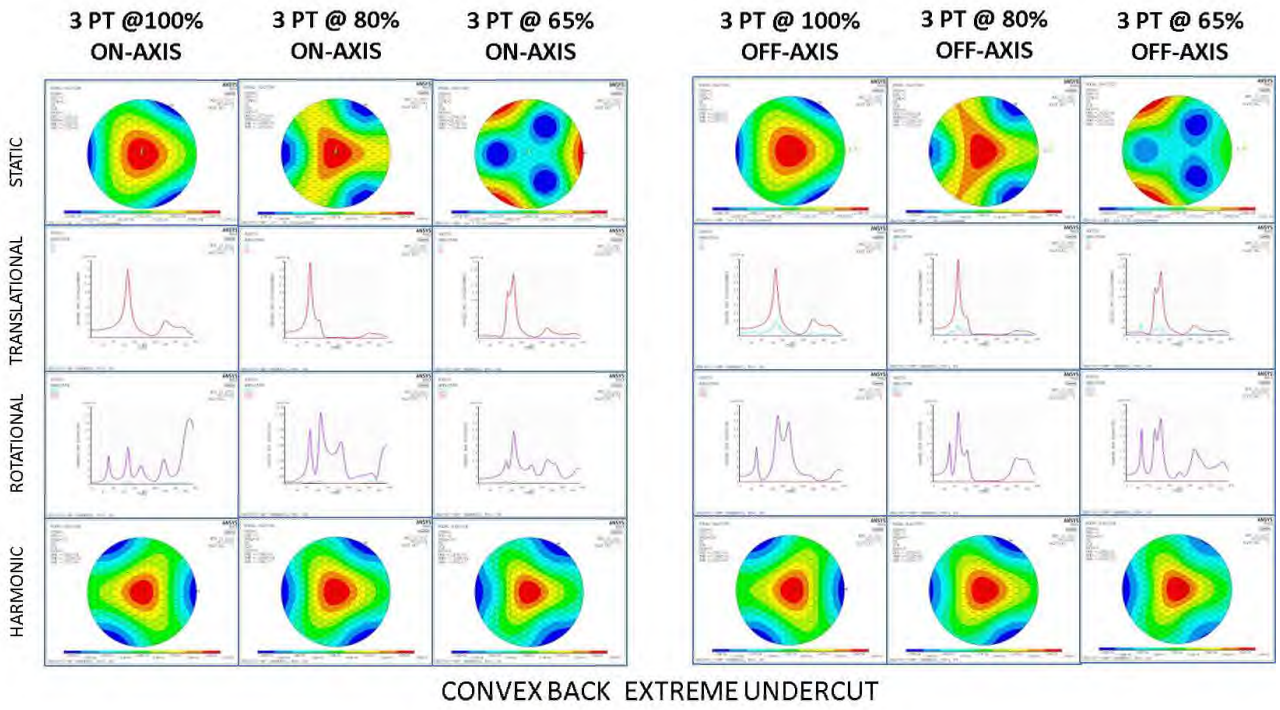

Figure B-9: Zerodur Trade Study #9

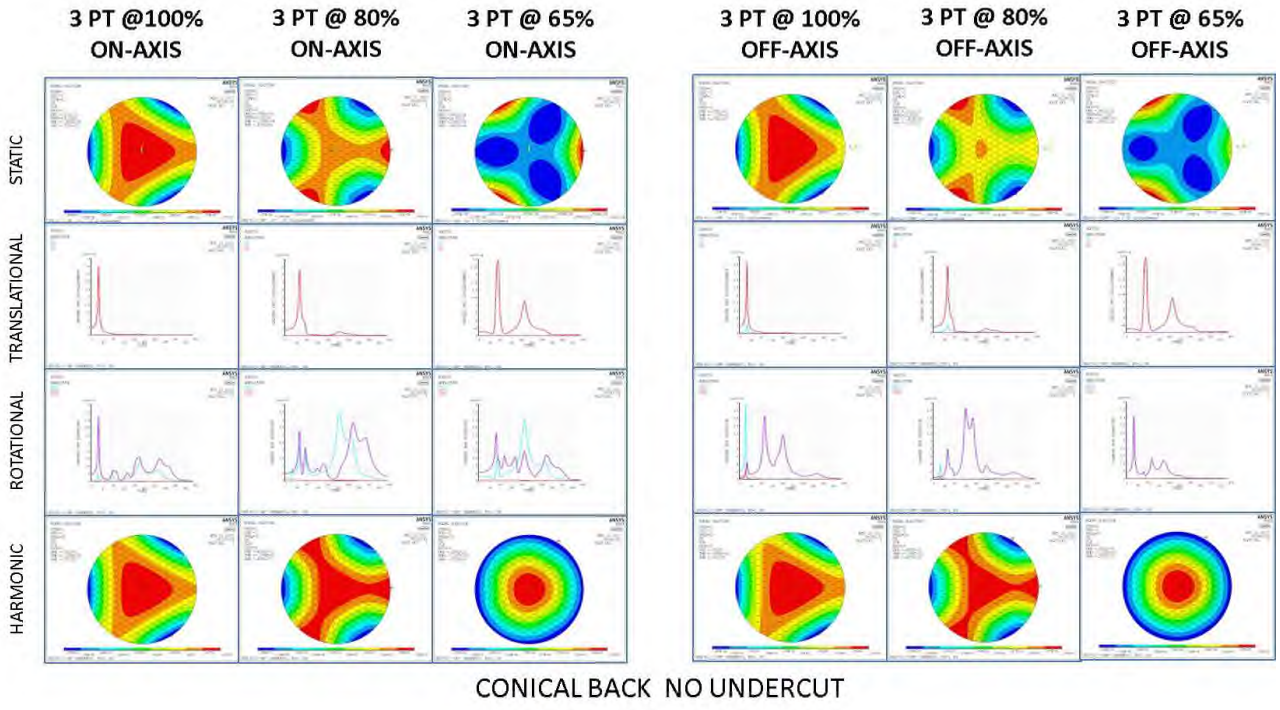

Figure B-10: Zerodur Trade Study #10

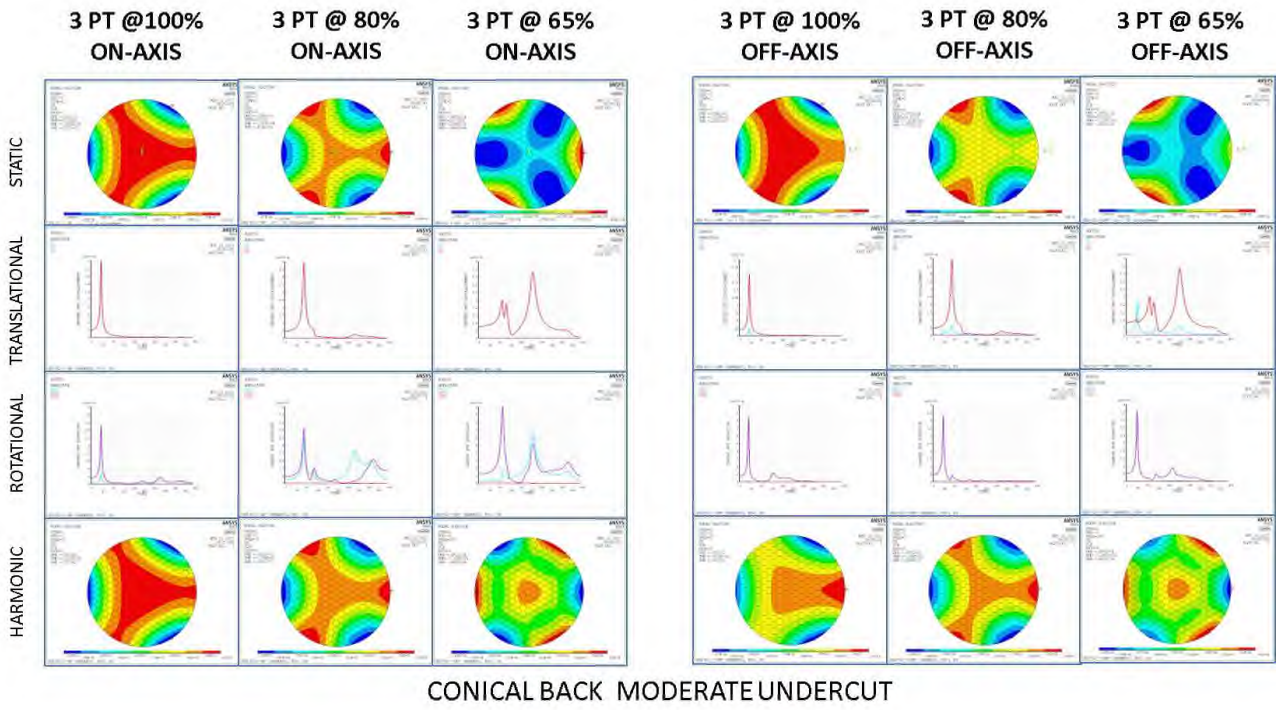

Figure B-11: Zerodur Trade Study #11

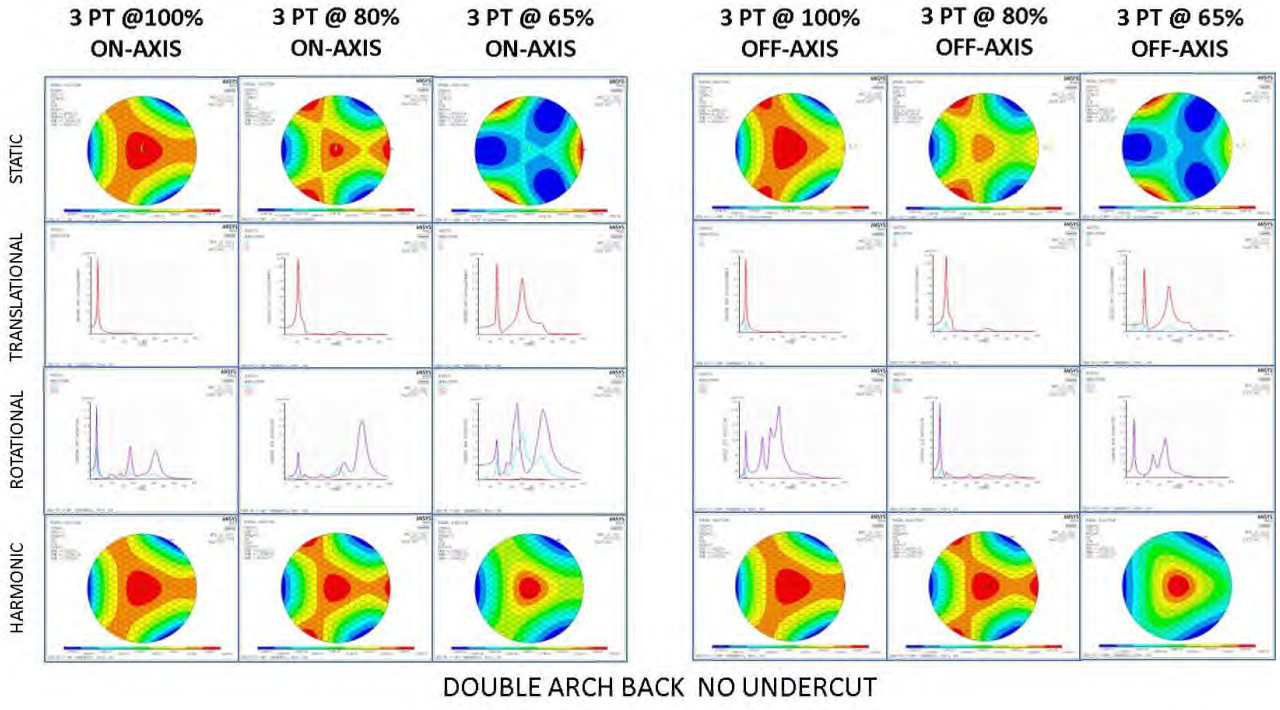

Figure B-12: Zerodur Trade Study #12

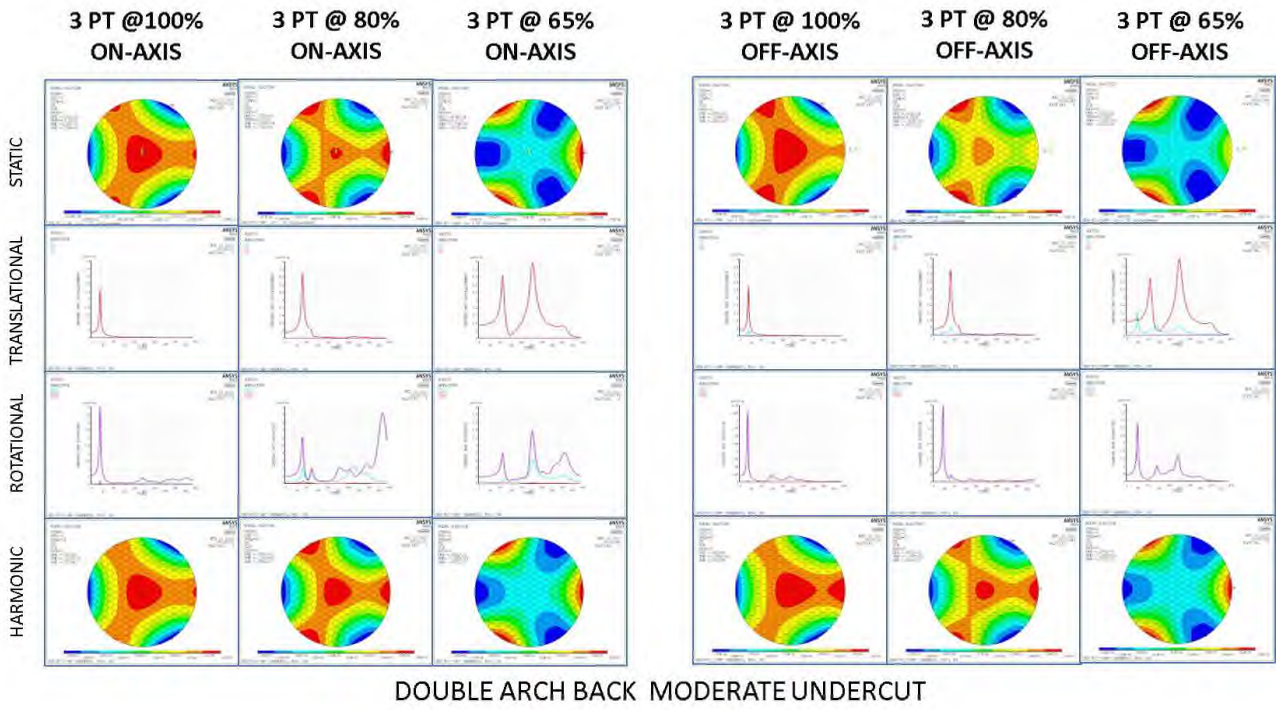

Figure B-13: Zerodur Trade Study #13

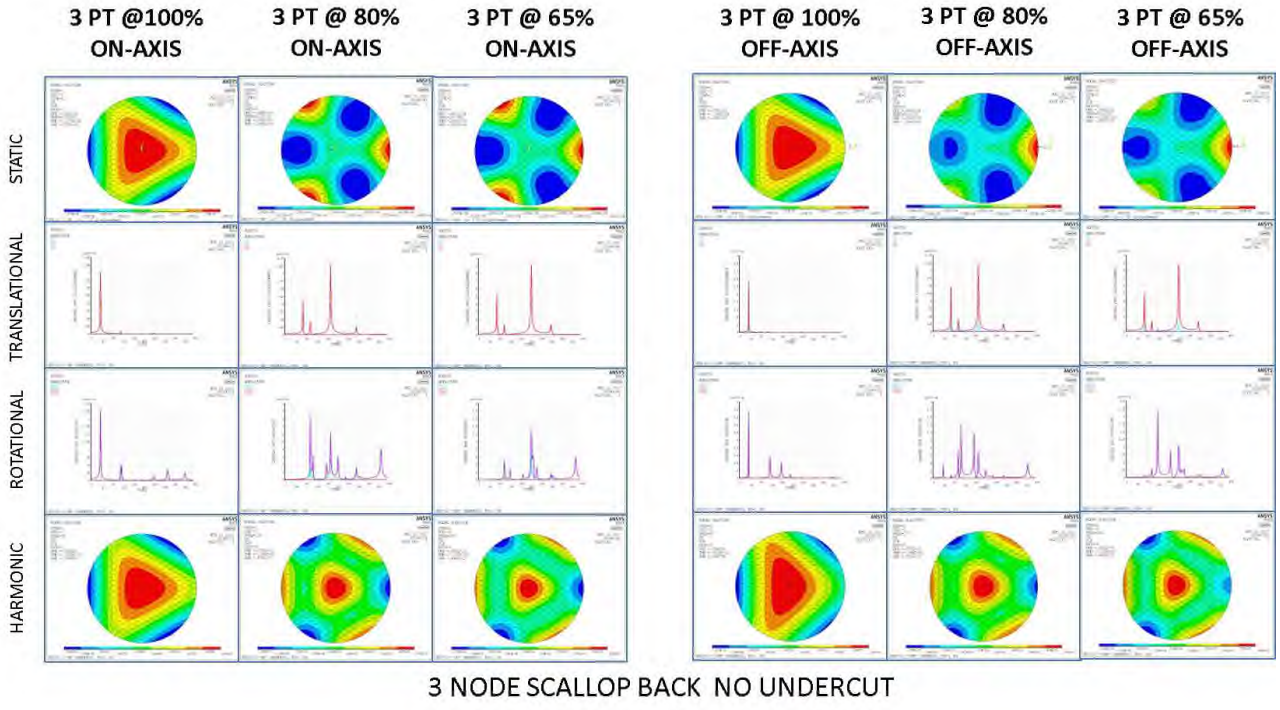

Figure B-14: Zerodur Trade Study #14

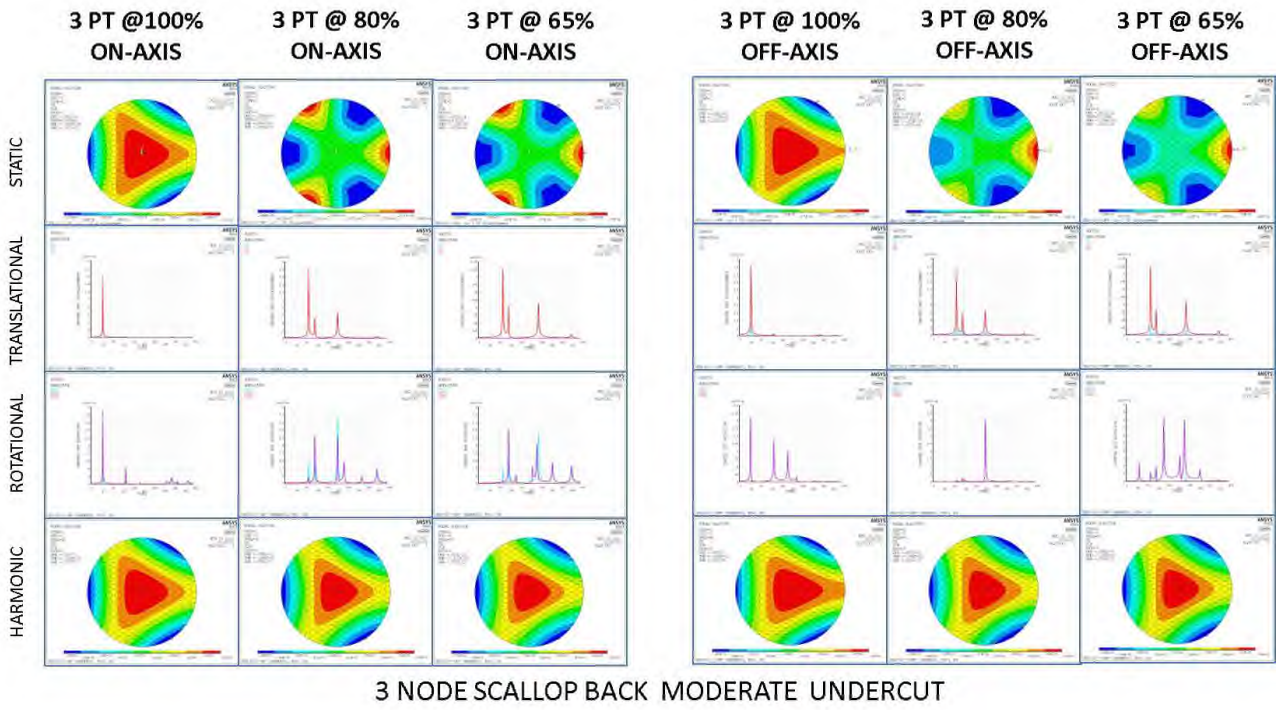

Figure B-15: Zerodur Trade Study #15

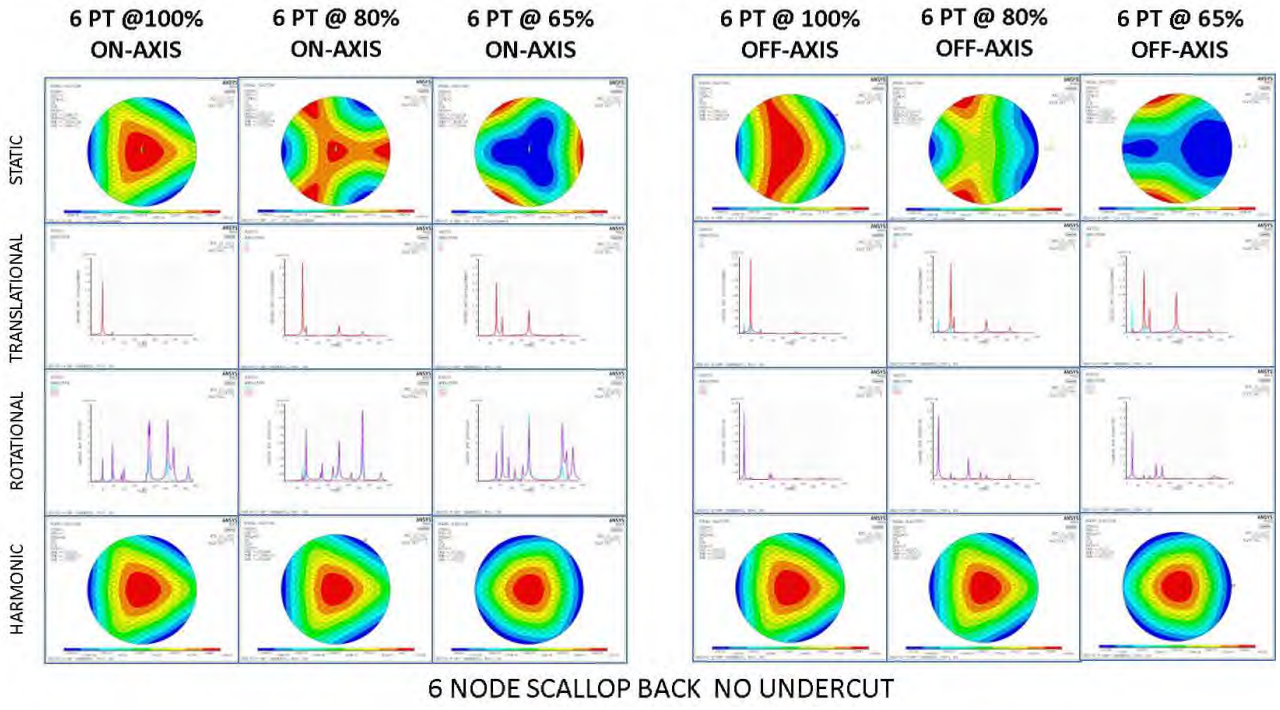

Figure B-16: Zerodur Trade Study #16

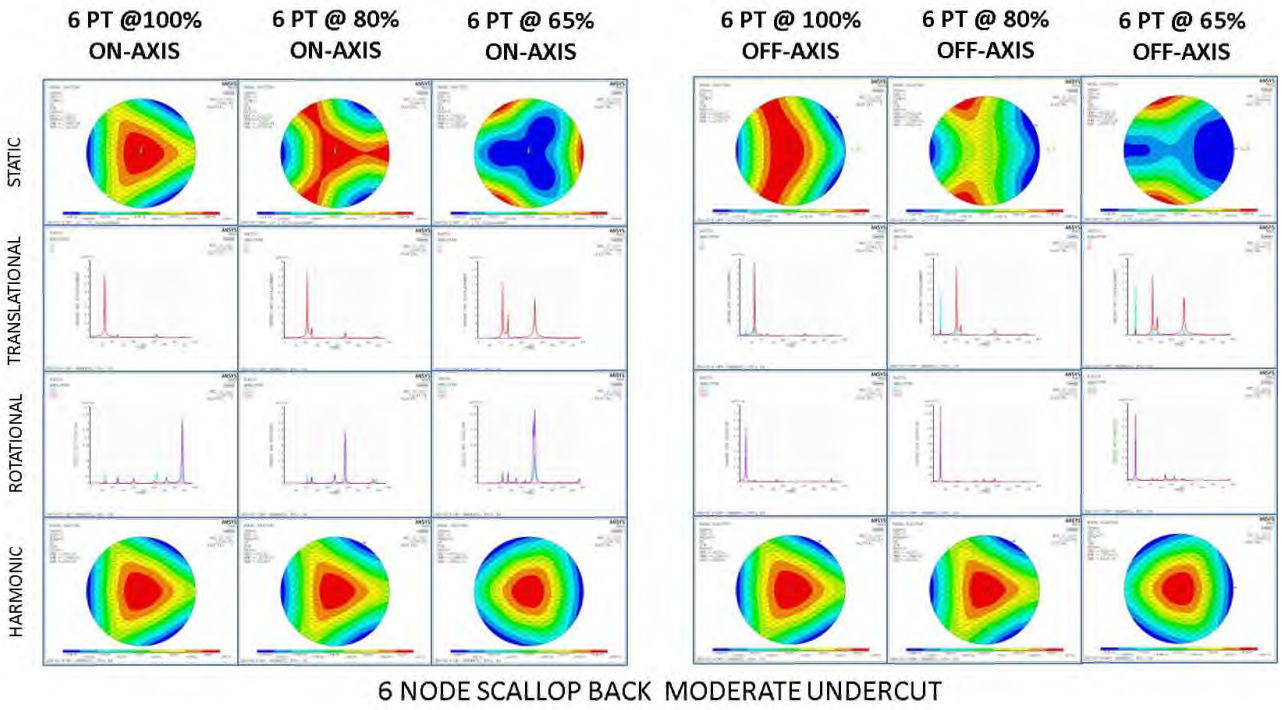

Figure B-17: Zerodur Trade Study # 17

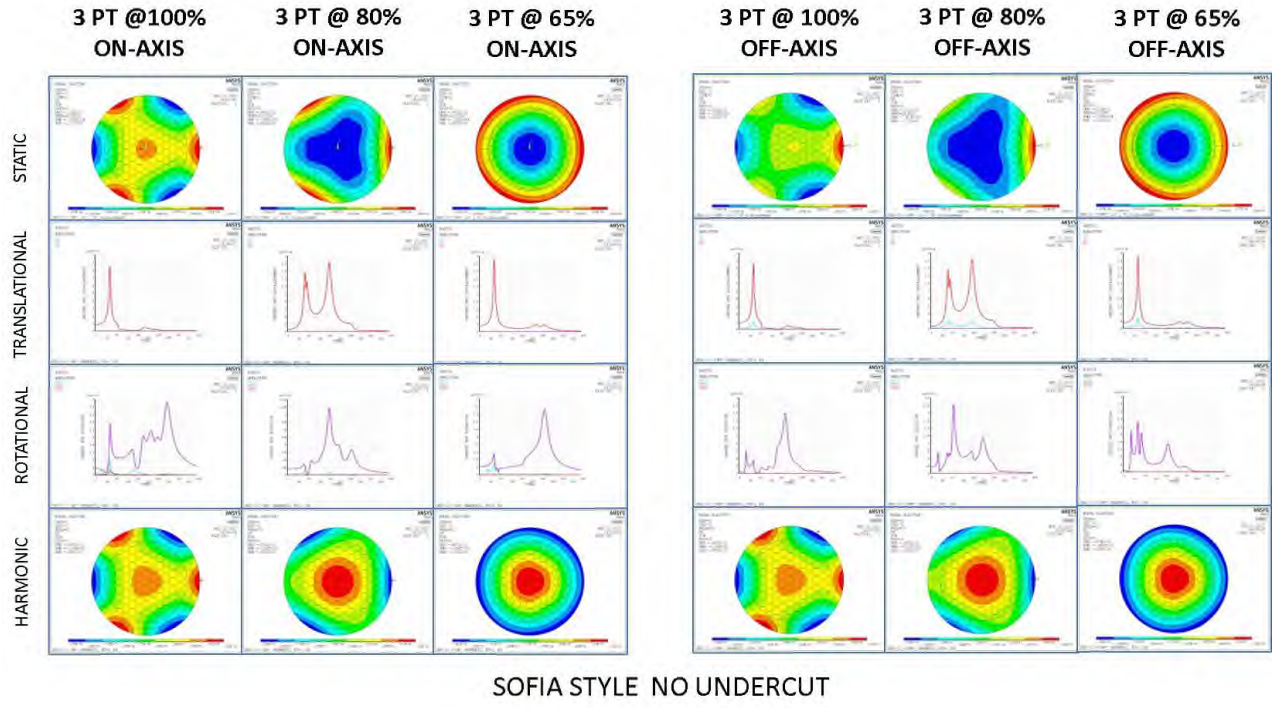

Figure B-18: Zerodur Trade Study #18

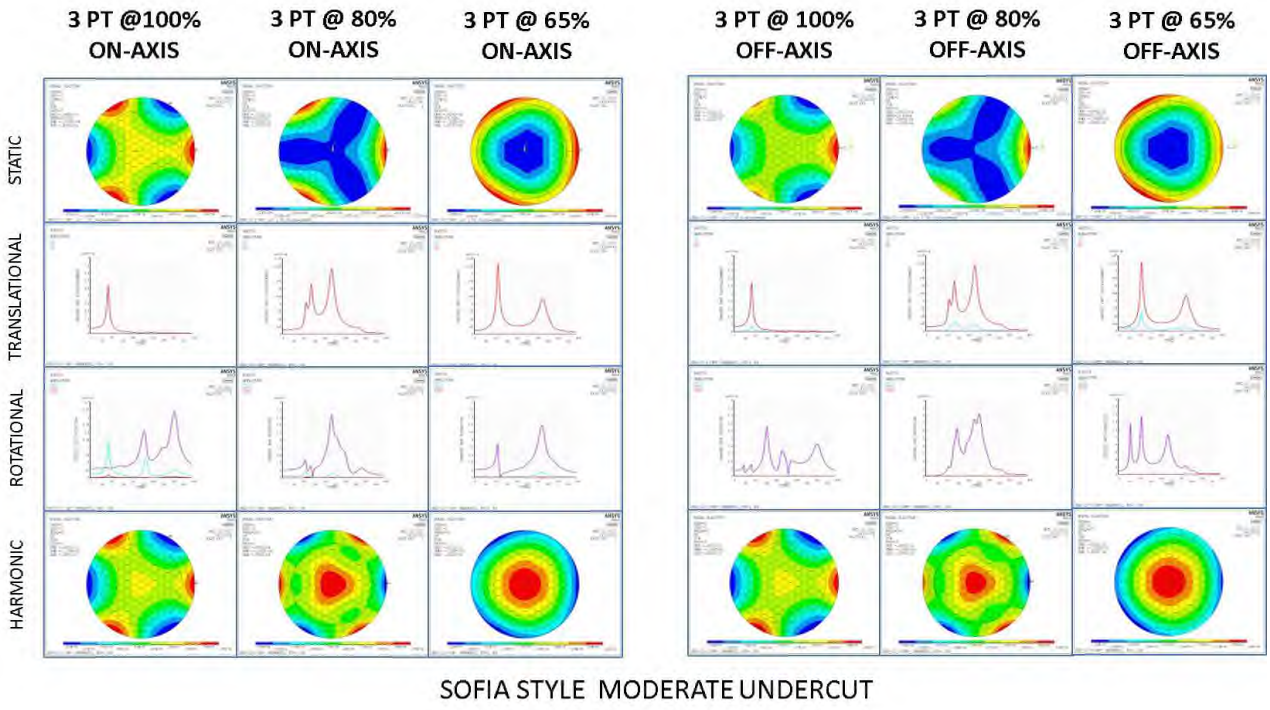

Figure B-19: Zerodur Trade Study #19

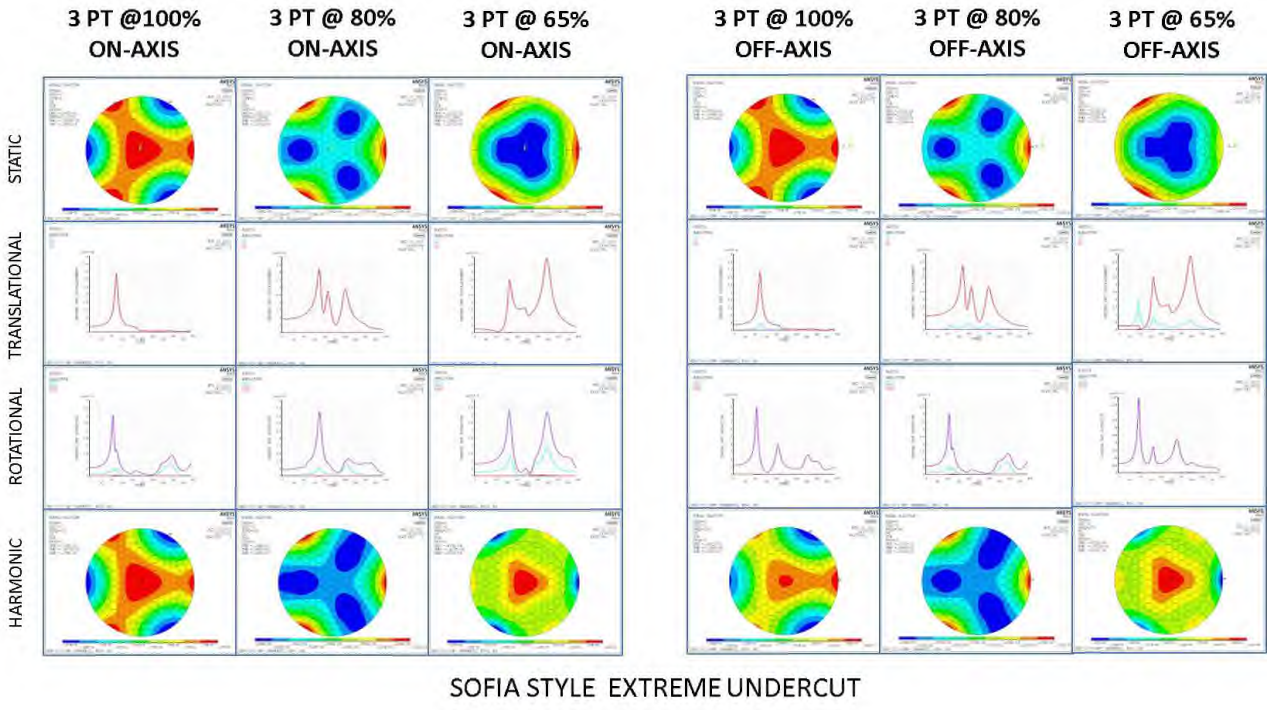

Figure B-20: Zerodur Trade Study #20